BRIGHAM YOUNG UNIVERSITY

GEOLOGY
S T U D I E S

GEOLOGICAL SOCIETY OF AMERICA

FIELD TRIP GUIDE BOOK

1997 ANNUAL MEETING • SALT LAKE CITY, UTAH

PART 2 TWO

EDITED BY PAUL KARL LINK AND BART J. KOWALLIS

VOLUME 42 • 1997

MESOZOIC TO RECENT GEOLOGY OF UTAH

Edited by
Paul Karl Link and Bart J. Kowallis

BRIGHAM YOUNG UNIVERSITY GEOLOGY STUDIES

Volume 42, Part II, 1997

CONTENTS

A Publication of the
Department of Geology
Brigham Young University
Provo, Utah 84602

Editor

Bart J. Kowallis

Brigham Young University Geology Studies is published by the Department of Geology. This publication consists of graduate student and faculty research within the department as well as papers submitted by outside contributors. Each article submitted is externally reviewed by at least two qualified persons.

Cover photos taken by Paul Karl Link.

Top: Upheaval Dome, southeastern Utah.
Middle: Lake Bonneville shorelines west of Brigham City, Utah.
Bottom: Bryce Canyon National Park, Utah.

ISSN 0068-1016
9-97 700 23870/24290

Preface

Guidebooks have been part of the exploration of the American West since Oregon Trail days. Geologic guidebooks with maps and photographs are an especially graphic tool for school teachers, University classes, and visiting geologists to become familiar with the territory, the geologic issues and the available references.

It was in this spirit that we set out to compile this two-volume set of field trip descriptions for the Annual Meeting of the Geological Society of America in Salt Lake City in October 1997. We were seeking to produce a quality product, with fully peer-reviewed papers, and user-friendly field trip logs. We found we were bucking a tide in our profession which de-emphasizes guidebooks and paper products. If this tide continues we wish to be on record as producing "The Last Best Geologic Guidebook."

We thank all the authors who met our strict deadlines and contributed this outstanding set of papers. We hope this work will stand for years to come as a lasting introduction to the complex geology of the Colorado Plateau, Basin and Range, Wasatch Front, and Snake River Plain in the vicinity of Salt Lake City. Index maps to the field trips contained in each volume are on the back covers.

Part 1 "Proterozoic to Recent Stratigraphy, Tectonics and Volcanology: Utah, Nevada, Southern Idaho and Central Mexico" contains a number of papers of exceptional interest for their geologic synthesis. Part 2 "Mesozoic to Recent Geology of Utah" concentrates on the Colorado Plateau and the Wasatch Front.

Paul Link read all the papers and coordinated the review process. Bart Kowallis copy edited the manuscripts and coordinated the publication via Brigham Young University Geology Studies. We would like to thank all the reviewers, who were generally prompt and helpful in meeting our tight schedule. These included: Lee Allison, Genevieve Atwood, Gary Axen, Jim Beget, Myron Best, David Bice, Phyllis Camilleri, Marjorie Chan, Nick Christie-Blick, Gary Christenson, Dan Chure, Mary Droser, Ernie Duebendorfer, Tony Ekdale, Todd Ehlers, Ben Everitt, Geoff Freethey, Hugh Hurlow, Jim Garrison, Denny Geist, Jeff Geslin, Ron Greeley, Gus Gustason, Bill Hackett, Kimm Harty, Grant Heiken, Lehi Hintze, Peter Huntoon, Peter Isaacson, Jeff Keaton, Keith Ketner, Guy King, Mel Kuntz, Tim Lawton, Spencer Lucas, Lon McCarley, Meghan Miller, Gautam Mitra, Kathy Nichols, Robert Q. Oaks, Susan Olig, Jack Oviatt, Bill Perry, Andy Pulham, Dick Robison, Rube Ross, Rich Schweickert, Peter Sheehan, Norm Silberling, Dick Smith, Barry Solomon, K.O. Stanley, Kevin Stewart, Wanda Taylor, Glenn Thackray and Adolph Yonkee. In addition, we wish to thank all the dedicated workers at Brigham Young University Print Services and in the Department of Geology who contributed many long hours of work to these volumes.

Paul Karl Link and Bart J. Kowallis, Editors

New explorations along the northern shores of Lake Bonneville[1]

CHARLES G. (JACK) OVIATT
Department of Geology, Kansas State University, Manhattan, Kansas 66506

DAVID M. MILLER
U.S. Geological Survey, 345 Middlefield Road, Menlo Park, California 94025

ABSTRACT

This field trip begins in Salt Lake City and makes a clockwise circuit of Great Salt Lake, with primary objectives to observe stratigraphic and geomorphic records of Lake Bonneville. Stops include Stansbury Island, Puddle Valley, gravel pits at Lakeside and the south end of the Hogup Mountains, several stops in Curlew Valley and Hansel Valley, and a final stop at the north end of Great Salt Lake east of the Promontory Mountains. Stratigraphic observations at gravel-pit and natural exposures will be linked to interpretations of lake-level change, which were caused by climate change. Evidence of paleoseismic and volcanic activity will be discussed at several sites, and will be tied to the lacustrine stratigraphic record. The trip provides an overview of the history of Lake Bonneville and introduces participants to some new localities with excellent examples of Lake Bonneville landforms and stratigraphy.

INTRODUCTION

Objectives

The objectives of this trip are to (1) show key new localities along the northern shores of late Pleistocene Lake Bonneville in an area where unusually complete preservation of Lake Bonneville deposits and landforms provides new insights into the lake's evolution; (2) visit some classic sites; and (3) provide an overview of Lake Bonneville and selected Holocene lake features in the context of climate history and neotectonics. Lake Bonneville is one of the best studied late Pleistocene pluvial lakes and its record of waxing and waning is a powerful paleoclimate proxy. This paleoclimate record plays a fundamental role in paleoecology studies and serves as a benchmark for testing local, regional, and global climatic hypotheses. Geomorphic features of the lake serve as vital markers for recording neotectonic events because both age and paleohorizontal can be established with shoreline features. As a result, deposits and landforms of Lake Bonneville provide valuable clues for understanding Quaternary volcanism and faulting in northwest Utah. In addition, modern hazards, from flooding to contamination and salt-water intrusion, are best understood within the context of the complete Holocene record of Great Salt Lake. Our approach will be to look at a number of Lake Bonneville features around Great Salt Lake, including at classic sites and newly discovered sites, and set this in the context of climate, neotectonic, and hazard themes.

Regional description

Lake Bonneville was the largest of numerous late Pleistocene pluvial lakes that formed in the Great Basin, a division of the Basin and Range physiographic province characterized by playas, lakes, and internally draining rivers in hydrologically closed basins interspersed with north-trending mountains that includes western Utah, most of Nevada, and parts of adjoining states. Although much of the northeastern part of the Great Basin was occupied by Lake Bonneville at its highstand (fig. 1), the Bonneville basin now is marked by mountains separated by wide arid valleys, and few perennial streams. The three broadest lowlands are Great Salt Lake, the Great Salt Lake Desert, and the Sevier Desert. Thresholds between these lowlands provided some

[1]With a contribution by Dorothy Sack, Department of Geography, Ohio University, Athens, Ohio 45701.
With amino-acid results from Darrell Kaufman, Department of Geology, Utah State University, Logan, Utah 84322.

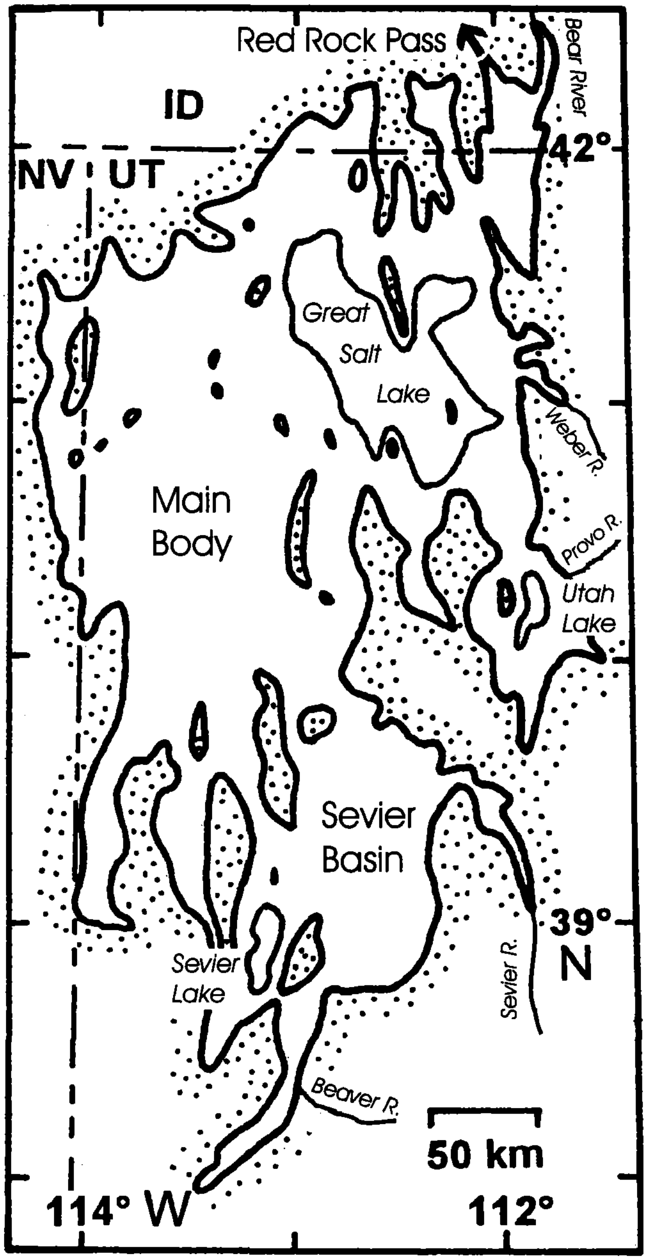

Figure 1. Map of Lake Bonneville at the Bonneville shoreline stage (15 ka).

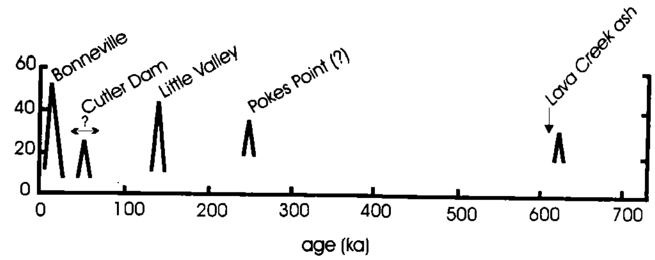

Figure 2. Major Quaternary lake cycles in the Bonneville basin (modified from Figure 3 of Machette and Scott, 1988), determined primarily from outcrop data.

controls on lake levels, but climatic factors provided the primary influence on the lake's budget of water influx and evaporation. Rivers on the eastern side of the basin contributed most of the water to the lake, because they drained the largest and highest mountains.

The topography of the northeastern part of the Great Basin was formed by normal faulting that created alternating uplifted and downthrown north-trending structural blocks, referred to as basins and ranges. This topography started developing during the Pliocene or latest Miocene, about 5 to 7 Ma (Miller et al., 1992). Many of the ranges in northwestern Utah are bounded by normal faults that had Quaternary activity, and some have experienced Holocene activity (Christenson et al., 1987). The principal Holocene fault activity is along the Wasatch Front on the Wasatch fault (and related faults), but faults under Great Salt Lake and north of Great Salt Lake in and near Hansel Valley also ruptured during the Holocene. This western zone of recent faulting also contains Quaternary volcanoes (Miller et al., 1995), reinforcing the possibility that it is a zone of magmatism and rifting (Smith and Luedke, 1984) (see Stop 7 and fig. 24 below).

Late Cenozoic precursors to Lake Bonneville

The term Lake Bonneville is used here to refer to the last major late Pleistocene lake in the Bonneville basin, which existed between about 28 and 12 ka (Oviatt et al., 1992; Oviatt, 1997). Earlier Quaternary lake cycles have been documented in the basin (fig. 2), but Lake Bonneville and Holocene lakes are far better understood because the older lake deposits have been largely obliterated by erosion or buried by younger lake deposits and alluvium. Long cores of sediments from the floor of the Bonneville basin collected by A. J. Eardley and his colleagues during the 1950s and 1960s (Eardley and Gvosdetsky, 1960; Eardley et al., 1973) contain evidence of a number of pre-Bonneville Quaternary lakes that occupied the basin, although reexamination of these cores by Oviatt and R.S. Thompson (unpublished) indicates fewer major lake cycles than Eardley originally interpreted from the cores. On this field trip we will get a glimpse of deposits of several pre-Bonneville lake cycles (at the Lakeside gravel pit; Stop 3), but we will spend most of our time on deposits and landforms of Lake Bonneville.

Lake Bonneville studies

Although evidence of a greatly expanded lake was noted by the Spaniards Dominguez and Escalante in 1776, the

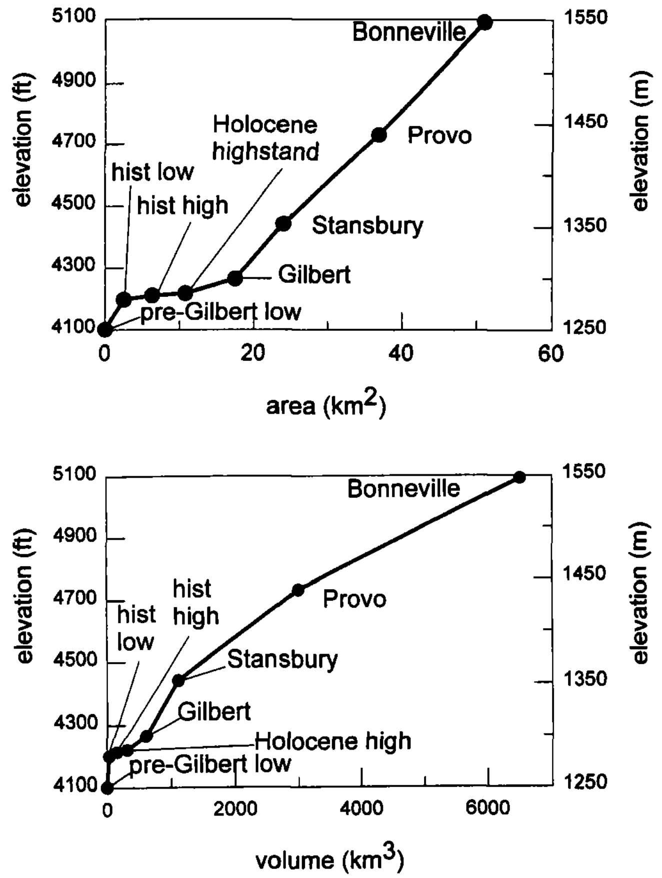

Figure 3. Graphs of surface area and volume vs. elevation in the Bonneville basin. Data from Currey (1990, Fig. 16). Data points are for shorelines of Lake Bonneville and for high and low stands of Great Salt Lake.

significance of shorelines far above the level of modern Great Salt Lake wasn't realized until Fremont and Stansbury explored the basin in the 1840s and 1850s (Sack, 1989). Other federally sponsored surveys during the late 1800s led to the masterful work of Grove Karl Gilbert, who named the ancient lake, Lake Bonneville, and spent many years studying its geology, geomorphology, and stratigraphy. USGS Monograph 1 (Gilbert, 1890) is the full report of Gilbert's studies and illustrates his amazing abilities as a scientist and observer.

Since the publication of Monograph 1 many people have studied Lake Bonneville, and ideas about its history have evolved considerably (see reviews by Machette and Scott (1988), and Sack (1989)). It is worth noting, however, that after more than a century, during which Gilbert's hypotheses have been repeatedly tested, many of his ideas and conclusions have withstood scrutiny and today stand as the solid framework of a robust body of knowledge about Lake Bonneville.

OVERVIEW OF LAKE BONNEVILLE

General Concepts

At its maximum about 15 ka, Lake Bonneville had a depth of over 300 m, a surface area of 51,000 km^2, and a volume of approximately 6500 km^3 (fig. 3). It had numerous bays, arms, peninsulas, and islands. The large rivers that emptied into the lake along the high mountains to the east produced tremendous volumes of clastic sediment, which dominate the stratigraphic records in valleys along the mountain fronts (Lemons et al., 1996). Over most of the area of Lake Bonneville, however, where no rivers discharged sediment, the source of shorezone clastic sediment was alluvium and weathered bedrock on mountain flanks, and impressive constructional shoreline features, such as spits, barriers, and tombolos (some of which will be seen on this trip) were deposited. In distal areas where clastic input was small, the dominant fine-grained facies is marl.[2] Typically, coarser grain sizes were deposited close to shore where wave energy was high, and fine-grained facies (marl) were deposited offshore, but there are exceptions to these general rules that depend on local geomorphic controls. For instance, dropstones from shore ice or rootballs of rafted trees are common in certain settings of the marl, and some fine-grained sediments were deposited where wave energy was low and fine-clastic input was high.

A schematic stratigraphic column of a typical white marl section specific to a deep-water, or low-altitude, location is shown in fig. 4. At higher altitudes, early and late parts of the history are not represented. Refer to fig. 5 to place the stratigraphic units mentioned here in the chronology of Lake Bonneville. Coarse-grained littoral deposits at the base grade upward into sandy marl and laminated marl (early transgressive-phase and Stansbury marl), which grades upward into more massive marl (deposited during the deepest-water phases) that generally has a lower clastic content, and in many places is pink or dark green in color. The massive marl has an abrupt upper contact with a sandy laminated unit (the Bonneville flood unit) that in many places contains abundant reworked ostracodes. The sandy laminated unit

[2] Gilbert named one of the Lake Bonneville stratigraphic units the White Marl, and the fine-grained calcareous facies of the Bonneville Alloformation is still referred to informally as the white marl. On this field trip we will examine a number of exposures of the (stratigraphic unit) white marl, most of which will fit the definition of marl ("a soft, grayish to white, earthy or powdery, usually impure calcium carbonate precipitated on the bottoms of present-day freshwater lakes and ponds largely through the chemical action of aquatic plants ... the calcium carbonate content may range from 90% to less than 30%" [Bates and Jackson, 1987]). In Lake Bonneville, marl was deposited even during the deepest stages, calcium carbonate was probably precipitated in the epilimnion, and minute crystals of calcite or aragonite settled to the lake bottom. In places the (stratigraphic unit) white marl contains over 80% calcium carbonate, but in other places it may consist of calcareous sand, depending on the local input of clastic debris.

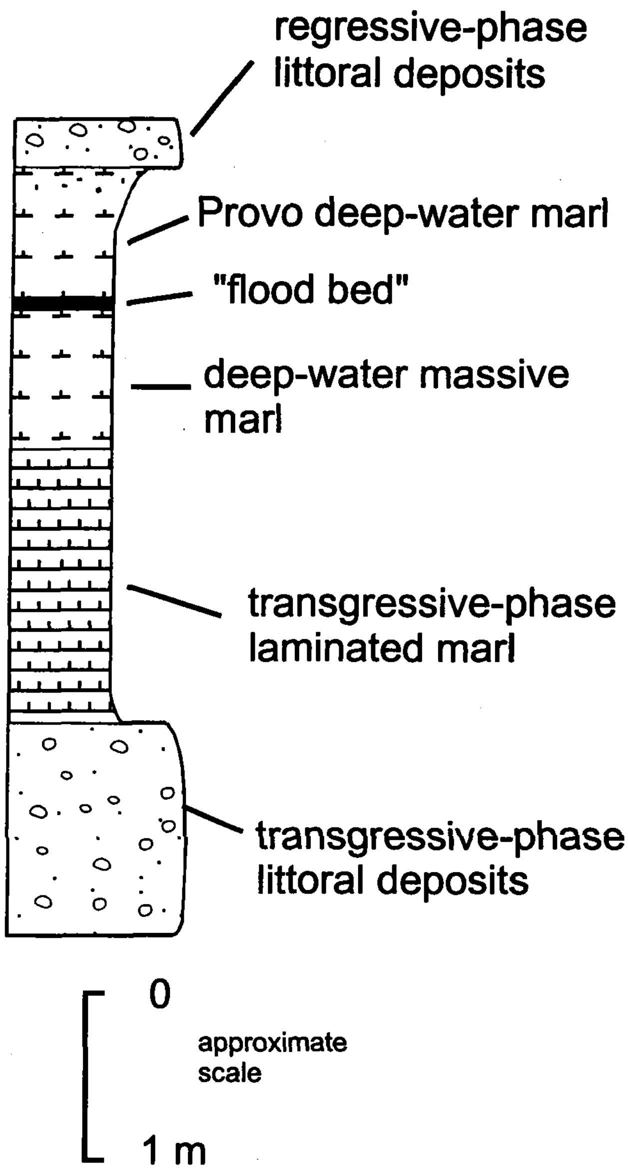

Figure 4. Generalized stratigraphic column of the white marl showing facies that are likely to be encountered at a low-elevation site in the main body of Lake Bonneville (modified from Oviatt et al., 1994, fig. 3). Typical ostracodes in the three main facies are as follows. Post-Bonneville flood (Provo deep-water marl): Cytherissa lacustris, Candona caudata, Candona adunca, Limnocythere ceriotuberosa, Candona eriensis *(?); Deepest-water phase (deep-water massive marl):* Candona adunca, Limnocythere ceriotuberosa, Candona caudata*; Early transgressive phase (transgressive-phase laminated marl):* Limnocythere staplini, Candona caudata. *Ostracode abbreviations used in subsequent figures:* ***genus*** **Candona***:* C. adunca = *Ca,* C. caudata = *Cc,* C. eriensis = *Ce,* C. decora = *Cd,* C. rawsoni = *Cr;* ***genus*** **Limnocythere***:* L. staplini = *Ls,* L. ceriotuberosa = *Lc,* L. sappaensis = *Lsa;* ***genus*** **Cytherissa***:* C. lacustris = *Cyl.*

grades upward into another massive marl unit (deposited during the Provo stage and initial regression), which grades upward into coarse-grained sediments (of the final regression). Fossil ostracode faunas in these subunits of the white marl are distinctive (fig. 4), and are very helpful in intrabasin correlations (as the water chemistry changed with changes in lake volume and level, the ostracode assemblages changed [Forester, 1987; Thompson et al., 1990]). Marl chemistry (carbonate content, relative proportions of different carbonate minerals, oxygen and carbon isotopes) also varies systematically and will be discussed at several stops on the field trip. For instance, for marl precipitated in during periods of relatively low lake level, the percentage of total carbonate, the aragonite/calcite ratio, and the relative values of oxygen and carbon isotopes are relatively high (Oviatt et al., 1994; Oviatt, 1997).

Some of the shorelines of Lake Bonneville have been mapped throughout the basin (Gilbert, 1890; Currey, 1982; Currey et al., 1984), but many shorelines do not have regional signatures, and can be mapped for only short distances along individual mountain fronts. Two of the mapped shorelines (Bonneville and Provo) are prominent because they formed during periods of overflow at the basin rim (near Red Rock Pass, Idaho), but other mapped shorelines (Pilot Valley, Stansbury, Gilbert) were not threshold controlled, and are difficult to confidently identify in many places. On this field trip we will observe good examples of all five of the above-mentioned shorelines, as well as numerous examples of unnamed shorelines.

As Gilbert (1890) noted, the major shorelines of Lake Bonneville are not horizontal on a regional scale, but are bowed upward in the interior of the basin—the Bonneville shoreline is 74 m higher in the Lakeside Mountains than at the basin rim (Red Rock Pass), and the Provo shoreline is bowed upward a maximum of 59 m (fig. 6). Gilbert correctly attributed the deformation to isostatic rebound following the removal of the Lake Bonneville water load, and subsequent work has refined Gilbert's shoreline mapping and the modeling of the isostatic response (see Crittenden, 1963; Currey, 1982; Bills and May, 1987).

History

Lake Bonneville began to rise from elevations similar to modern Great Salt Lake (~1280 m; 4200 ft) after about 28 ka (all ages discussed in this guidebook, except for historic dates, are in radiocarbon years B.P.) (fig. 5). The Pilot Valley shoreline, which was first mapped in the vicinity of Pilot Valley (Miller, 1990), was produced at about the level of the regressive-phase Gilbert shoreline sometime after 28 ka. The Pilot Valley shoreline is prominent in a number of areas in northwest Utah, but has not yet been mapped through-

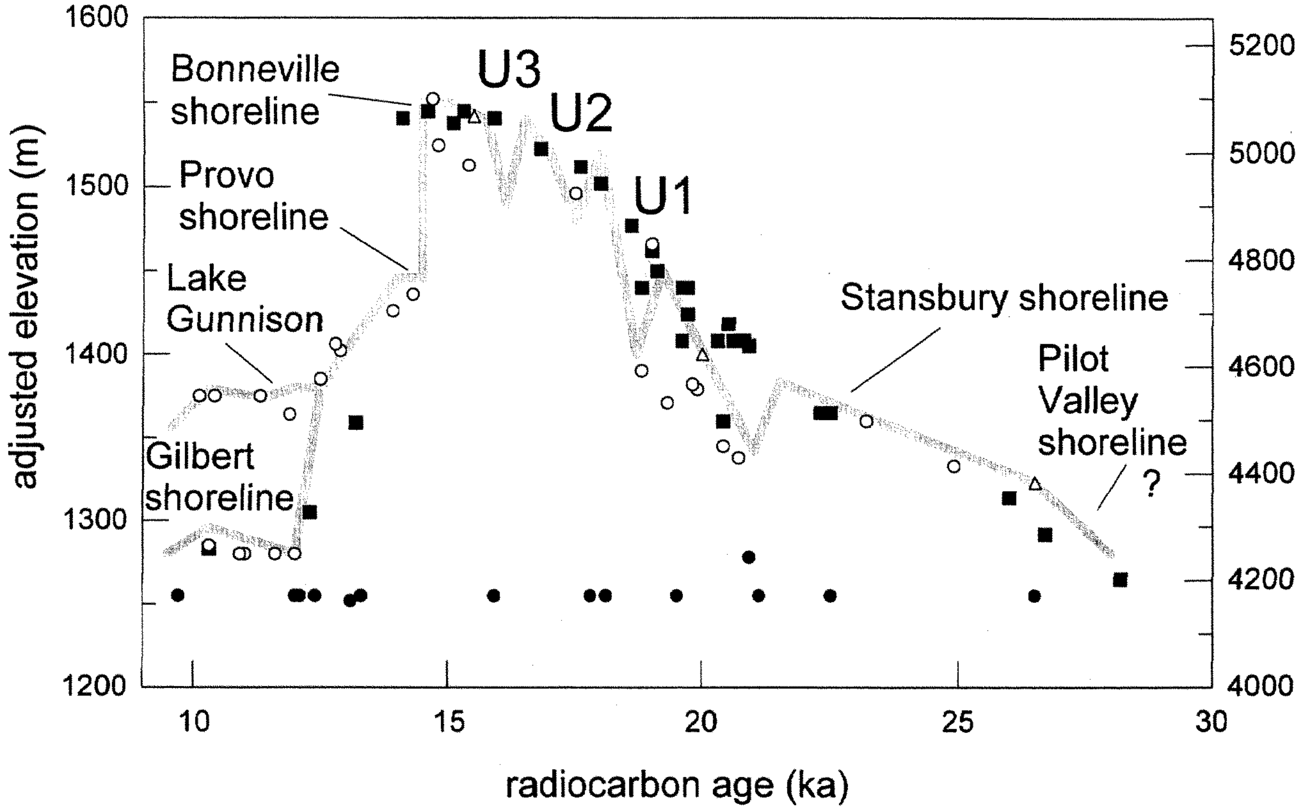

Figure 5. Lake Bonneville time-altitude curve modified from Oviatt et al., (1992, fig. 3) and Oviatt (1997, fig. 2). Elevations are adjusted for the effects of isostatic rebound in the basin (Oviatt et al., 1992), and ages are in radiocarbon years. Open circles are carbonate radiocarbon samples (shell, tufa), solid circles are disseminated organic carbon samples, solid squares are wood or charcoal samples, and open triangles are basaltic ashes. U1, U2, and U3 are unnamed transgressive-phase fluctuations.

out the Great Salt Lake basin. Lake Bonneville had reached an elevation of about 1340 m (4400 ft) by 26.5 ka (fig. 5). Later in the transgressive phase the lake experienced a series of fluctuations, each on the order of 30–50 m (Stansbury, U1, U2, U3), before reaching its highest stage at the Bonneville shoreline about 15 ka. The lake briefly overflowed (probably less than 500 yr) near Red Rock Pass, ID, as the Bonneville shoreline formed, catastrophically dropped about 100 m when the alluvial-fan threshold failed about 14.5 ka, then continued to overflow noncatastrophically at a new stable threshold during the formation of the Provo shoreline. During regression below the Provo shoreline the lake dropped past an intrabasin threshold, referred to as the Old River Bed threshold, and the lake was divided into two separate lakes, one in the Sevier Lake basin (Lake Gunnison), and one in the Great Salt Lake basin, which received overflow from the Sevier basin. The Gilbert shoreline formed in the Great Salt Lake basin during a moderate rise between 11 and 10 ka.

The Bonneville shoreline ranges widely in degree of development and preservation depending on local geomorphic controls, such as wave energy and direction, substrate resistance, slope, and sediment supply. The Provo shoreline is commonly the best developed, ~100 m (~330 ft) below the Bonneville. Provo and Stansbury shorelines are marked by prominent drapes of tufa and cemented beachrock, each with a marl "dump" below. The Gilbert shoreline is sporadically developed, and where present typically has a relatively fresh-looking appearance. The Pilot Valley shoreline is exposed sporadically across northern Utah at low elevations, and as the earliest regionally developed shoreline, is an important reference frame for measuring isostatic deformation.

Basaltic volcanic ash has been useful in Lake Bonneville stratigraphic studies (Oviatt and Nash, 1989; Miller et al., 1995). The Hansel Valley ash (discussed below) was erupted from an unidentified vent in northern Utah about 26.5 ka. Several other basaltic ashes (Pahvant Butte, Tabernacle Hill, and Pony Express) have been described in the Sevier Desert region in the southern part of the Bonneville basin.

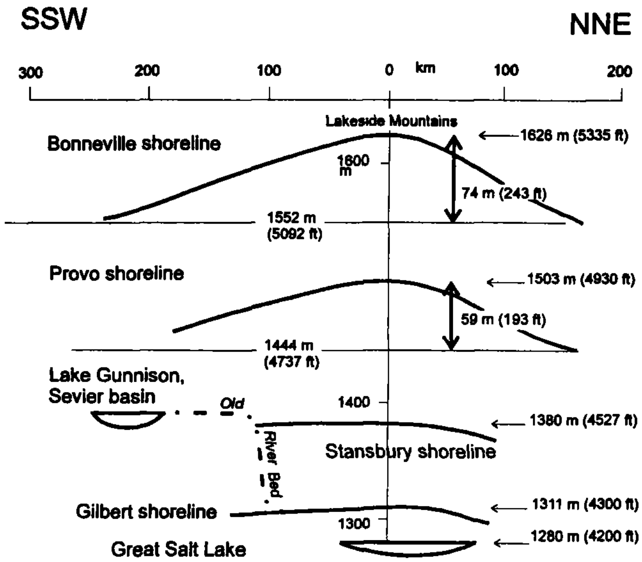

Figure 6. Isostatic rebound of Bonneville, Provo, Stansbury, and Gilbert shorelines. Modified from Currey (1990, fig. 13). The fine lines labeled 1552 m and 1444 m associated with the Bonneville and Provo shorelines, respectively, represent the unrebounded elevations of those shorelines. Lake Gunnison, in the Sevier basin, overflowed into the Great Salt Lake basin during the development of the Gilbert shoreline. The Lakeside Mountains are near the center of the Lake Bonneville water load, and therefore, the shorelines are rebounded the greatest amount in this area.

Unresolved questions

A number of questions about Lake Bonneville history are still being pursued. The transgression of Lake Bonneville, and all the falling-lake events (or regressions), such as the Stansbury, U1, U2, U3, the post-Provo regression, and the post-Gilbert regression, were caused by climate change in the basin. For most of its history the lake was hydrographically closed so that changes in lake level reflect shifts in the water budget of the basin. The Bonneville cycle as a whole was correlative with marine oxygen-isotope stage 2, and each of the major falling-lake events was correlative with the abrupt termination of an iceberg rafting event in which large quantities of debris were deposited on the floor of the North Atlantic Ocean (Oviatt, 1997). The iceberg-rafting events were associated with global climate changes (Bond and Lotti, 1995). Therefore, the Bonneville-basin water budget was sensitive to global climate change on time scales ranging from at least 10^5 to 10^3 yr. The rapid response of Great Salt Lake to El Niño forcing during the 1980s suggests that the basin has the potential to yield high-resolution (decadal?) paleoclimate records if complete, undisturbed sedimentary sequences can be identified and sampled. More work is needed (and underway) to help refine the timing and magnitude of water-budget shifts during the late Pleistocene and Holocene.

Although the timing of the final regression of Lake Bonneville is known to have occurred between about 14 and 11 ka, the details of the regression are poorly understood because of the paucity of suitable datable materials in meaningful contexts. The isostatic response of the basin to loading and unloading is still being refined (Bills and May, 1987). For example, the altitude of the Gilbert shoreline varies from place to place in a way that is not easily predicted by isostatic models. It is higher on the northwestern edge of the basin (4260 ft [1298 m] from the Pilot Range along the Utah-Nevada stateline to Curlew Valley) than elsewhere along north shore (4250 ft; 1295 m).

Other unanswered questions include: (1) Where was the Hansel Valley ash eruptive center? See more discussion below—locating the vent is important in assessing regional geologic hazards. (2) The Pilot Valley shoreline (~4275 to 4295 ft; 1303–1309 m), which formed early in the transgressive phase, has not been studied in detail: was its development regional in extent, and what is its age and paleoclimatic significance? (3) Was the rise to Stansbury very rapid, and were there significant lake-level fluctuations between the time of eruption of the Hansel Valley ash and the Stansbury oscillation? (4) What is the origin of the double shorelines at the Provo level, and how did isostatic rebound immediately after the Bonneville Flood affect shoreline development at the Provo?

OVERVIEW OF GREAT SALT LAKE

Great Salt Lake is a shallow, highly saline lake in a hydrologically closed basin, which fluctuates largely as a result of climatic and human-induced influences (see Gwynn, 1980; and Arnow and Stephens, 1990). A pair of thresholds north and south of the Newfoundland Mountains control overflow to the Great Salt Lake Desert at ~4217 ft (1285 m) altitude (Currey et al., 1984). At the average historical lake level (4202 ft; 1280 m), maximum depth is roughly 35 ft (11 m) and areal extent is 1800 mi^2 (4600 km^2) (Currey et al., 1984). The lake lies in an arid basin, and input is mainly from rivers draining mountains east of the lake. Principal stream inflow is from the Bear, Weber, and Jordan Rivers (fig. 9); this inflow is roughly double the direct contribution to the lake from precipitation. The shores of the lake typically have broad shallow mud flats that grade laterally to steeper areas, with the result that moderate lake-level fluctuations can produce either dramatic shoreline changes across the flats or very little shoreline change along steep slopes.

Prehistoric Great Salt Lake

The shoreline record that postdates the Gilbert-age lake deposits gives some information on major Holocene high-

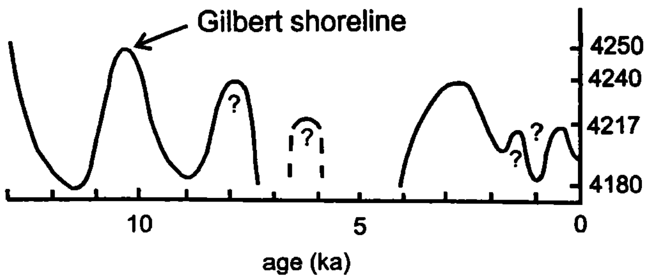

Figure 7. Holocene history of Great Salt Lake modified from Currey et al., (1984; see also Murchison, 1989).

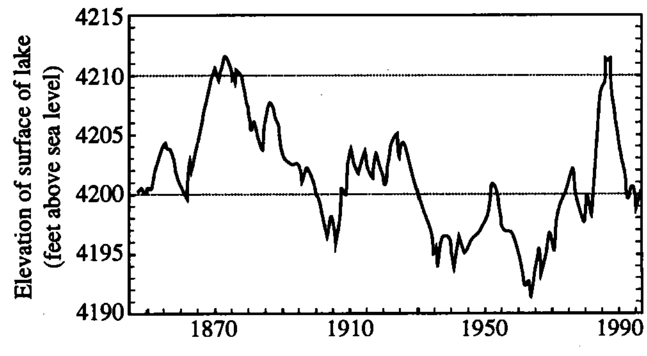

Figure 8. Historical fluctuations of the surface altitude of the southern part of Great Salt Lake. Data from the U.S. Geological Survey, 1996 Web Site.

stands of Great Salt Lake (fig. 7). At Locomotive Springs on the north shore of Great Salt Lake, a wave-cut notch at 4240 ft and a gravel beach at 4230 ft may be regressive shorelines of the Gilbert Stage but more likely are distinct Holocene lake highstands. A sand and gravel beach at 4218 ft rests on Holocene lake muds and represents one of the Holocene high stands of Great Salt Lake. Elsewhere along the north shore of Great Salt Lake 4240-ft and 4220-ft beaches are very common. Currey et al., (1988) described evidence that a 4221-ft shoreline formed between 2.5 and 2.0 ka. Some stands higher than the 4217-ft thresholds have taken place during the late Holocene, including the Little Ice Age highstand about 400 years ago (Currey et al., 1984). Atwood (1994) has been studying how the elevations of Great Salt Lake shorelines are affected by processes such as wind-generated lake-level changes, wind seiches, earthquake seiches, and diking or other human activities. An understanding of these geomorphic processes is important for accurate reconstructions of paleolake levels, and for assessing geologic hazards associated with rises in lake levels.

Historic lake levels

Great Salt Lake typically has 1- to 3-foot annual variation in lake level caused by seasonal variations in evaporation and influx. The hydrograph (fig. 8) for recordings at the southern end of the lake illustrates longer-term variation in lake levels, including the historic highs in the early 1870s, and in 1986–1987 (both rises reached almost to 4212 ft), and low in 1963 (4191 ft) (Mabey, 1986; Arnow and Stephens, 1990).

The Southern Pacific Railroad causeway bisecting the lake from Lakeside to Ogden artificially controls lake level. Most of the fresh water enters the south arm of the lake, and construction of the causeway in the 1950s, and modification in the 1980s, has caused lake levels in the northwest arm to be lower than in the south arm by several feet. In addition, the north arm has much higher salinity and slightly lower water levels. Several openings in the causeway allow water from the south arm to flow to the north at the surface, although dense saline water from the north arm also flows southward through the causeway openings.

The high lake levels caused by floods of the 1980s were probably similar to the those of the 1870s, although the first lake-level gage was installed in 1875, so the pre-1875 levels are estimates (Mabey, 1986). In the 1980s, the lake rose rapidly during a five year period (1982–1986) from about 4200 ft to almost 4212 ft (reported as 4211.85 ft) during 1986, and then dropped just as rapidly to its present level. The rate of rise and fall during this flood event was greater than 2 ft per year, despite significant human water consumption. Similar rates for past recorded rises and declines in lake level demonstrate the rapidity with which lake levels change. Most population growth in the region took place during a time when the lake was below its average level, and the roads and buildings constructed at low altitudes and were considerably damaged during the lake rise of the 1980s. To help control the damaging effects of high lake levels, a pumping plant was constructed in the southern Hogup Mountains to pump water from the lake to shallow basins in the Great Salt Lake Desert, which together acted as a huge evaporation basin (U.S. Geological Survey, 1987). Pumping during 1987 flooded roughly 600 mi^2 (1700 km^2) west of the Newfoundland Mountains.

Shorezone features

Oolitic sand is currently forming in shallow water around most of the margins of Great Salt Lake (Eardley, 1938; Gwynn and Murphy, 1980), except where clastic deposition and fresher water dominate near the deltas of the Bear and Jordan Rivers. In places, oolitic sand is reworked into eolian dunes at the shoreline.

We will observe or pass close to a number of springs and marshes at the margin of the lake on this field trip. Most notable will be the marshes at the Public Shooting Grounds

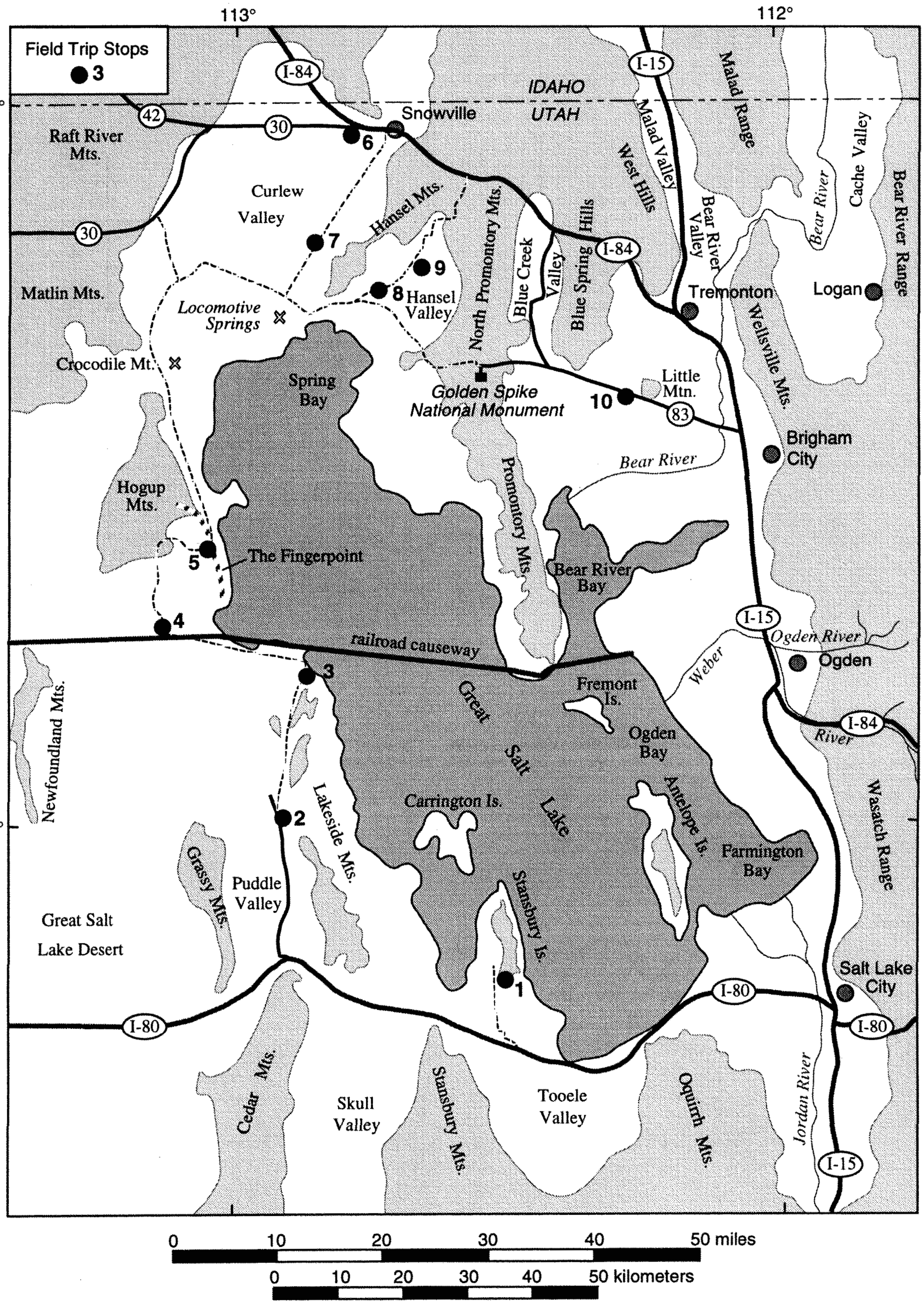
113°
112°
42°
41°
Field Trip Stops
3
I-84
I-15
IDAHO
UTAH
42
30
Snowville
Raft River Mts.
6
Curlew Valley
Hansel Mts.
7
9
8
Hansel Valley
Matlin Mts.
Locomotive Springs
Crocodile Mt.
North Promontory Mts.
Blue Creek Valley
Blue Spring Hills
West Hills
Malad Valley
Malad Range
Bear River Valley
Bear River
Cache Valley
Bear River Range
Tremonton
Logan
Wellsville Mts.
Spring Bay
Golden Spike National Monument
10
Little Mtn.
83
Brigham City
Bear River
Hogup Mts.
Promontory Mts.
5
The Fingerpoint
Bear River Bay
4
I-15
Ogden River
railroad causeway
3
Weber
Ogden
Fremont Is.
Great Salt Lake
Ogden Bay
I-84
River
Newfoundland Mts.
Carrington Is.
Antelope Is.
Farmington Bay
Wasatch Range
2
Lakeside Mts.
Grassy Mts.
Puddle Valley
Stansbury Is.
Great Salt Lake Desert
1
Salt Lake City
I-80
I-80
I-80
Cedar Mts.
Skull Valley
Stansbury Mts.
Tooele Valley
Oquirrh Mts.
Jordan River
I-15
0 10 20 30 40 50 miles
0 10 20 30 40 50 kilometers

at the north end of Bear River Bay. The Bear, Weber, and Jordan Rivers have built deltas along the east shore of Great Salt Lake.

Ecology and contamination

Despite its high salinity, Great Salt Lake supports a healthy ecosystem. Typical organisms include bacteria, blue-green algae, diatoms, brine shrimp, brine flies, and other aquatic insects. The lake itself, and the springs, deltas, and marshes at the margin of the lake, support a diverse avifauna.

Restricted circulation in the lake, due both to natural causes such as shallowness and long islands, and also to artificial barriers such as causeways, has served to concentrate contaminants in parts of the lake. Effective mitigation of contamination relies on traditional hydrologic principals such as knowing paths and rates of water input and circulation, and also a detailed knowledge of the chemistry and physical attributes of water in different parts of the lake. The unique waters may provoke unusual reactions with contaminants.

FIELD TRIP GUIDE

This trip will start and end in Salt Lake City, and will circle Great Salt Lake in a clockwise direction (fig. 9). We will use highway mileage markers for locating features during travel along major routes such as Interstate freeways, and give odometer mileage for roads off the major routes. We reset mileage to zero after each stop. Elevations are given in feet throughout the guidebook because the USGS 7.5-minute topographic quadrangles and benchmarks are in feet, and it is easier not to convert to meters (metric equivalents are given in parentheses).

DAY 1

Travel west from Salt Lake City on I-80.

Mile 104. To the north, Saltair recreation park lies on the gently sloping shore of Great Salt Lake. It was built in the early 1980s as a partial replication of the historic Saltair park, and promptly flooded during the 1982 to 1986 rise of the lake. Despite attempts to dike around the building, it was damaged extensively. Water stood at least 5 ft deep at the building. Note how far the lake has now receded. Kennecott's copper smelter lies south of the freeway. Marshes between the airport and Saltair are Holocene in age, and comprise part of the Jordan River distributary system.

Figure 9. Field trip stops and road route. Heavy lines are interstate highways; lighter lines are paved highways; dashed lines are graded gravel roads. Average shoreline for Great Salt Lake (4202 ft) is shown. Mountains (shaded) are outlined by the Provo shoreline. Adapted from Currey et al., (1984).

Mile 93. In this vicinity both I-80 and the parallel railroad north of the highway were raised during the mid-1980s as the lake rapidly rose to its highstand of almost 4212 ft during the early summers of 1986 and 1987. Note fenceposts still partly submerged.

Mile 84. Exit here (Grantsville exit). Set mileage to zero at stop sign. Turn right (north) and follow paved road west and north through several bends.

0.5	Pavement ends. Cross railroad heading north.
4.2	Intersection; take left fork.
6.0	Crossroads. Turn right (east) and drive to floor of gravel pit. Shorelines are visible on the mountain facing us.

STOP 1. Stansbury shoreline on Stansbury Island.

We will examine exposures in Stansbury Gulch that show a section of the white marl and a wedge of tufa-cemented gravel that can be traced to the Stansbury shoreline. The exposures demonstrate that the Stansbury shoreline formed early in the lake history and that offshore stratigraphy can be linked to geomorphic features.

Cream-colored sandstone outcrops form the west ridge of the short, steep valley, and gray limestone, the east. The tufa-cemented prominent shoreline high on the sandstone outcrops is the Provo shoreline, and the fainter shoreline about half way between the gravel pit (at the base of the mountain) and the Provo shoreline is the Stansbury shoreline. Both shorelines also can be seen on the limestone ridge. Most gravel exposed in the gravel pit at the base of the mountain was deposited during the initial transgression of Lake Bonneville. In some parts of the gravel pit, the white marl can be seen overlying trasnsgressive-phase gravel near the top of the exposure; the marl is overlain by a few meters of cobbles, which were deposited during the rapid regression of the lake. The white marl was truncated in most places during this regression event.

Walk up Stansbury Gulch to the northeast. A jeep track traverses the east side of the valley and may be drivable as far as a pit in the diatomaceous marl. The stratigraphy and geomorphology of Stansbury Gulch have been described in several previously published guidebooks (see Currey et al., 1983; Green and Currey, 1988). Two or three thin sand beds in the diatomaceous marl in the lower parts of the gully exposures can be traced up slope into thicker sand and then into a thick wedge of tufa-cemented gravel that is coincident with the Stansbury shoreline (fig. 10). A radiocarbon age of 20.7 ka (Currey et al., 1983) determined on gastropods collected from the sand at the lower end of the gravel wedge, in addition to the stratigraphic relationships, indicates that the Stansbury shoreline formed during the

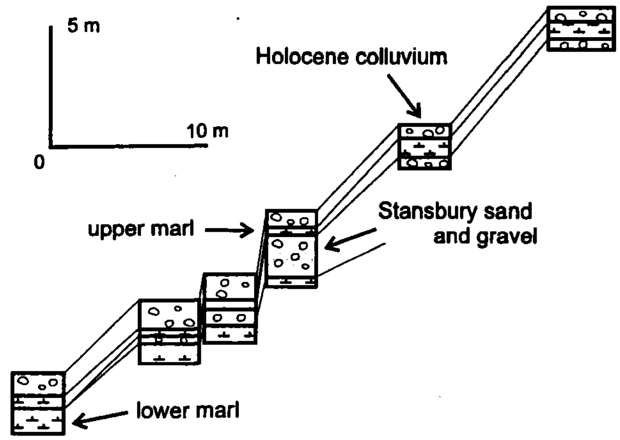

Figure 10. Stop 1—Schematic measured sections from the walls of the gully at Stansbury Gulch (modified from Currey et al., 1983, and Green and Currey, 1988). The sections are simplified into three main units: lower marl (below the Stansbury sand and gravel); Stansbury sand and gravel, including the thick tufa-cemented gravel; upper marl (which represents deep-water deposition between the time of development of the Stansbury shoreline and the regression below the Provo shoreline); and Holocene colluvium and debris flows. Two radiocarbon ages have been obtained from these sections: 20.7 ka on Pyrgulopsis (Amnicola) *shells from the Stansbury sand; and 24.9 ka on fine-grained $CaCO_3$ from the lower marl (Green and Currey, 1988).*

transgressive phase of Lake Bonneville during an oscillation in lake level. Stratigraphic and geomorphic interpretations from other locations in the Bonneville basin indicate that the total amplitude of the Stansbury oscillation was on the order of 45 to 50 m (150–165 ft) (Oviatt et al., 1990), although the evidence at Stansbury Gulch is insufficient in itself to demonstrate this.

The Stansbury oscillation is one of at least four major oscillations in lake level during the transgressive phase, each of which represents a significant change in water budget driven by climate change in the basin (fig. 5; Oviatt, 1997). For example, the Stansbury oscillation represented surface-area and water-volume changes of about 5000 km^2 and 1000 km^3, or relative changes of 18 and 50%, respectively (Oviatt et al., 1990). The other transgressive-phase oscillations had similar magnitudes, and represent climate changes probably associated with shifts in the mean position of storm tracks, which in turn were possibly determined by changes in the size and shape of the Laurentide ice sheet (Oviatt, 1997).

Retrace route to I-80 and enter freeway headed *west*. Near this location the 1000-ft (300-m) deep Burmester core was taken in 1970 by A.J. Eardley and his colleagues (Eardley et al., 1973). Eardley et al., attempted to correlate their interpretations of the Burmester core with other records of global climate change (European loess cycles and deep-sea records). However, a quick look at the core in 1993 convinced Oviatt and Bob Thompson (USGS) that Eardley et al., had missed the deposits of the deepest Quaternary lake in the basin (Lake Bonneville). That is, the white marl of Lake Bonneville is in the upper 6 ft of the core—an interval described by Eardley et al., as soil and interpreted as evidence of dry to shallow lake conditions. Therefore, in 1995 Oviatt and Thompson reexamined the Burmester core (and other cores taken by Eardley in the 1950s and 1960s) and concluded that the core contains a record of mudflat, eolian, and marsh sedimentation interspersed with a few units of marl deposited in deep lakes. The original paleomagnetic results, and recently obtained tephrochronology (Williams, 1994), provide age control for the past ~3.3 Ma. We concluded that there were only four major deep-lake cycles represented in the Burmester core, including Lake Bonneville, during the last 700 ka, in contrast to 17 deep-lake events interpreted by Eardley et al., (1973) for the same time interval. It is obvious that much more work needs to be done on the pre-Bonneville lacustrine history of the Bonneville basin.

Mile 81. Note the good view of the Bonneville, Provo, and Stansbury shorelines on the north end of the Stansbury Mountains, south of the freeway. The Provo shoreline is most prominent, and is draped by tufa-cemented beachrock.

Mile 77. Morton Salt plant on the right. Salt and other minerals extracted from Great Salt Lake brines are a key industry for the region.

Mile 62. Exit toward Lakeside. Reset mileage to zero at stop sign. Turn right and follow paved road toward Military area.

0.7 View over Puddle Valley, an internally-drained valley within the Bonneville basin. The two passes at the south end of Puddle Valley (one close by to the southeast and the other farther to the southwest where the freeway disappears over the horizon) are about 80 m below the Provo shoreline. The pass at the north end of the valley, which we will study at STOP 2, is lower.

4.6 Muddy marl outcrops are in the road cut; ostracodes indicate that the marl was deposited while Puddle Valley was innundated by Lake Bonneville.

4.9 Cross Lake Puddle shoreline. Currey (1980) noted and named this shoreline, which does not match regional shorelines of Lake Bonneville (see the contribution by Sack below).

8.9 Bonneville marl capped by eolian sand in exposures along the road.

13.1 Reduce speed as we approach a high mound with steep fronts north and west of the highway.

This is a mass of gravel (referred to by Sack [below] as an inflow feature or bar) that was emplaced into a lake in Puddle Valley. As the road climbs the gravel mound, note the steep southern front, and that the mound has an undulating surface, with swales filled by marl. The undulations are megaripple-like features, spaced 6 to 270 m apart. The marl is post-Stansbury in age, on the basis of ostracode studies.

14.4 Pass road on right to Wrathall Pass.

14.9 Turn right (east) on gravel road, pass under power lines.

15.1 Bear left to a gravel pit and pass sign "No trespassing–Government Property." Continue into pit and park on the left.

STOP 2. Stansbury oscillation and catastrophic inflow at Puddle Valley.

Lake Bonneville's Puddle Valley Connection
by
Dorothy Sack
Department of Geography, 122 Clippinger Labs
Ohio University, Athens, Ohio 45701

Puddle Valley is a 400-km^2 closed drainage basin located approximately 100 km west of Salt Lake City near the center of the Lake Bonneville basin. Its elevation ranges from 4317 ft (1316 m) on the valley floor to 6625 ft (2019 m) at the highest peak in the Lakeside Mountains, which form the valley's eastern boundary. Puddle Valley is completely surrounded by, that is, inset into, the Bonneville basin. For most of the last deep-lake cycle Puddle Valley was an integrated subbasin of Lake Bonneville and contained an arm of the great lake (Gilbert, 1890; Currey et al., 1984). Shoreline evidence reveals that an independent Lake Puddle (Currey, 1980) occupied the valley at least briefly after its re-isolation from Lake Bonneville (Sack, 1995), but today there is no naturally occurring perennial or intermittent surface water in the valley.

The lowest point on Puddle Valley's drainage divide lies in the unnamed pass through which the paved highway extends at the north end of the valley. The threshold has a modern elevation of about 4470 ft (1362 m), which is below the modern local elevations of all three major Lake Bonneville shorelines, the Bonneville (5330 ft; 1625 m), Provo (4925 ft; 1501 m), and Stansbury (~4530 ft; ~1380 m), and above the post-Bonneville Lake Puddle level 4390 ft (1338 m) (Currey, 1982; Sack, 1995). Puddle Valley became part of the Bonneville basin when Lake Bonneville spilled from the north over this threshold into Puddle Valley. The inflow event is marked in the pass by a 1.2-km long spillway that slopes to the south and by a distinctive landform, first noted by Currey (1980), that is preserved just beyond the end of the spillway in Puddle Valley.

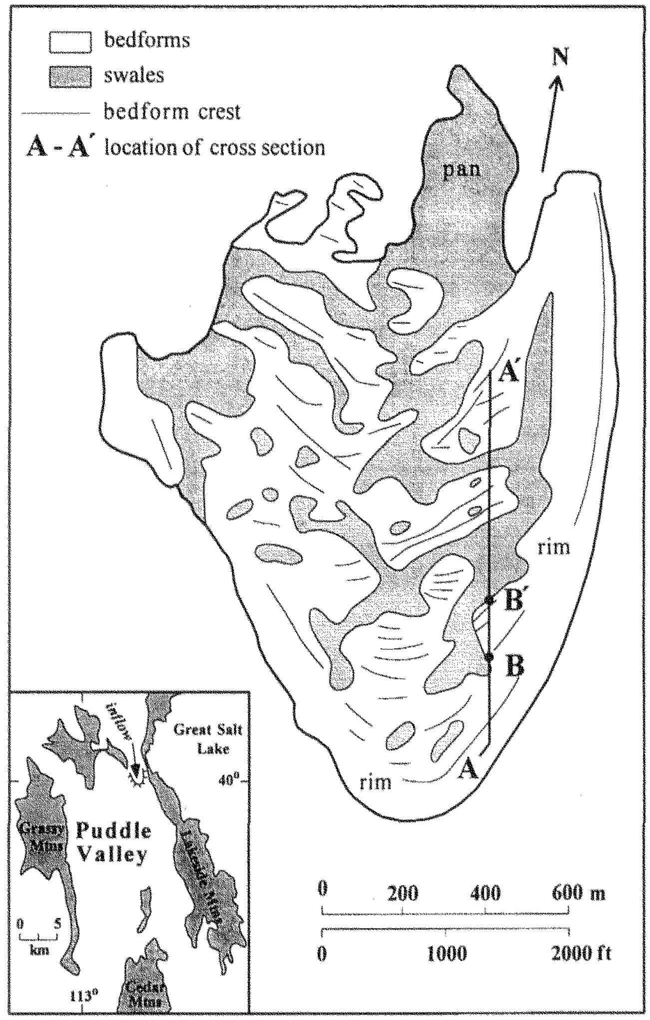

Figure 11. Planimetric map of the Puddle Valley inflow bar. The measured cross section from A-A′ appears in figure 12.

The Lake Bonneville inflow feature in Puddle Valley is a large-scale, tongue-shaped bar on which are found giant current ripples (fig. 11). The gravel bar, which is 1.5 km long and up to 1.2 km wide, consists of a pan on the up-current side bordered by a continuous lateral and lee-side rim. Elevations range from 4400 ft (1341 m) at the distal base of the bar to 4450 ft (1357 m) at the crest of the highest bedform. Along the highway road cut, the moderately asymmetrical giant current ripples range in height from 0.2 to 5.2 m, in length from 6 to 271 m, and in vertical form index (L/H) from 15 to 71 (fig. 12). The ripples consist of gravel cross beds that dip 9° to 24° towards Puddle Valley. Clasts sampled from 14 sediment pits dug in the bedforms had an average A axis of 10 cm and the overall ten largest clasts

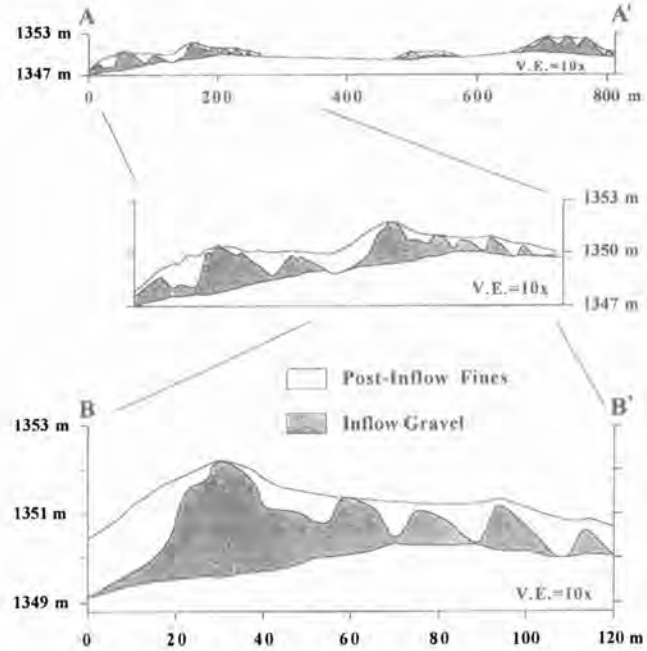

Figure 12. Measured cross section through giant current ripples on the Puddle Valley inflow bar.

Figure 13. Photo of gravel pit exposure at stop 2 (east of Puddle Valley threshold).

had an average A axis of 35 cm. The surface of the bar complex is mantled with Lake Bonneville white marl, clastic lacustrine fine-grained sediments, and postlacustrine eolian sandy silt.

The dimensions of the giant current ripples, size of constituent clasts, and presence within the bedforms of rip-up fragments of pre-Bonneville lacustrine marl (R.M. Forester, 1992, pers. comm.), tufa, and beachrock indicate that inflow was a high-velocity event accompanied by sudden catastrophic failure of the threshold. Because evidence of the Stansbury shoreline complex, which formed between about 22 and 20 ka (Oviatt et al., 1992), is found in Puddle Valley (Sack, 1995), the valley must have become part of the Bonneville lake basin before Stansbury shoreline time. Using the Lake Bonneville hydrograph (fig. 5) and the Puddle Valley threshold elevation, corrected for postlake hydroisostatic rebound (Currey and Oviatt, 1985), it is estimated that Lake Bonneville spilled into Puddle Valley and created the inflow bar about 25.8 ka and that the two basins re-isolated no later than about 12.2 ka.

[end of contribution from D. Sack]

Marl exposed in the wall of the gravel pit east of the PuddleValley threshold (fig. 13) is the upper, or post-Stansbury, marl as shown by the ostracode faunas. This indicates that the spits and barriers in the vicinity of the pass (fig. 14), on which the marl rests, are pre-Stansbury or Stansbury in age, and that the catastrophic inflow to Puddle Valley is also pre-Stansbury or Stansbury in age. Cross-bedded sand at the base of the exposure is overlain by about 65 cm (2 ft) of sandy marl. A carbonate hard ground in the upper part of the marl may mark the stratigraphic position of the Bonneville flood—marl and sand above this contact are coarser grained, and contain gastropods typical of Provo and post-Provo deposits (*Stagnicola* [formerly *Lymnaea*] and *Pyrgulosis* [formerly *Amnicola*]). A sample of gastropods collected from the sand directly above the marl yielded a radiocarbon age of 16,620 yr B.P. (Beta-100449). This apparent age, which is several thousand years older than expected, is inconsistent with the interpretation based on independent stratigraphic information (lithology, ostracodes, gastropods), and suggests that at least some of the dated gastropod shells were reworked from older deposits.

The hypothesis that some of the shells might be reworked is supported by amino acid analyses of a subsample of the gastropod shells. Darrell Kaufman (Utah State University, unpublished data) found potentially two different age groups of shells for each of the two genera. For instance, the average ratios of alloisoleucine to isoleucine for a total of twelve analyses are: for *Stagnicola*, (group 1) 0.113 ± 0.001, n=2 and (group 2) 0.133 ± 0.006, n=4; and for *Pyrgulopsis*, (group 1) 0.149 ± 0.002, n=4 and (group 2) 0.164 ± 0.004, n=2. Reworking was likely a common process in Lake Bonneville, especially in certain environments during the regressive phase of the lake, or during smaller-scale fluctuations.

Return to the paved road, reset mileage to zero, and turn right (north).

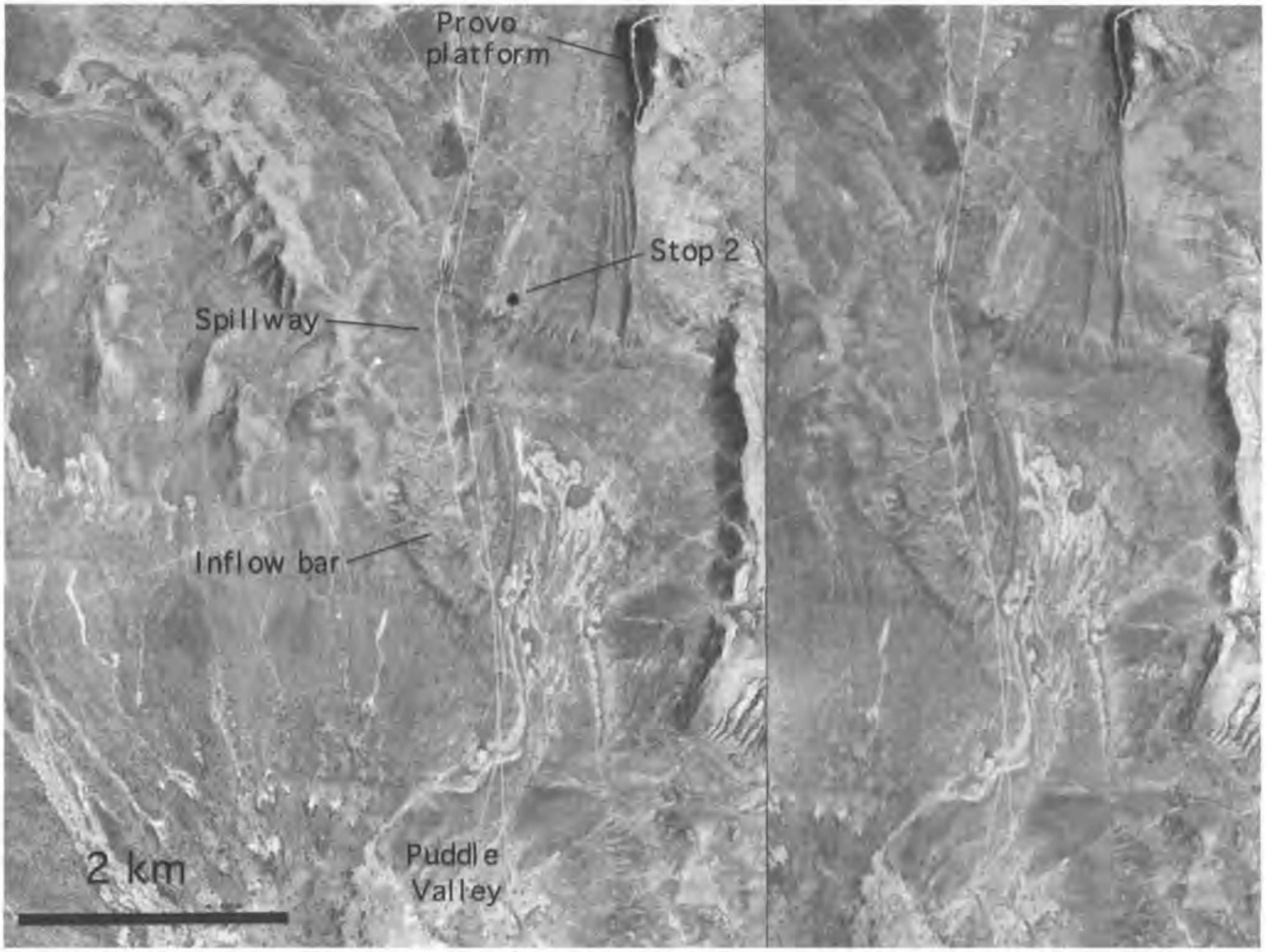

Figure 14. Stereo pair of Puddle Valley pass area. Aerial photographs were taken August 10, 1953.

0.5 Bear right on a gravel road. Paved road goes to military base.

7.5 The large tombolo on the skyline to the east is at an altitude between the Stansbury and Provo shorelines, just below the Provo.

8.4 Bear left at fork in road. Twin Hills (near Lakeside) lie in the distance to the north. Both have prominent Provo erosional platforms with sea stacks in their centers.

Homestead Knoll lies west of the road. Homestead and Cathedral caves, both in Homestead Knoll, have an important lacustrine and terrestrial record that is currently being studied by David Madsen (Utah Geological Survey) and colleagues.

12.9 Continue straight (north) on main road.

14.3 Turn right (east) on small gravel road toward pump house. Park about 150 ft past pump. Walk to edge of quarry (to the north).

STOP 3. Multiple barrier beaches at Lakeside quarry.

From the edge of the quarry, look east at the architecture and stratigraphy exposed at the east and south ends of the quarry where deposits of at least five lake cycles are exposed. The youngest of these is the Bonneville lake cycle, which is represented by a transgressive-phase gravel barrier overlain by the white marl. Underlying the Bonneville deposits is a sequence of at least four pre-Bonneville lacustrine units that are ripe for study (fig. 15).

Unit 1 is poorly exposed at the base of the east wall of the pit. It consists of coarse foreset gravel and minor carbonate mud that fills spaces between clasts. We know virtually nothing about the lake cycle created that it.

Unit 2 consists of horizontally bedded gravel that thickens to the south into foreset gravel of a barrier beach. On the lagoon side of the barrier, and exposed in a bench that trends west from the east wall of the pit, the barrier is conformably overlain by a marl unit that dips to the south (fig. 16). The

Figure 15. Photo of deposits on east wall of Lakeside gravel pit. Numbers refer to gravel units discussed in the text (under Stop 3).

marl is about 0.8 m thick, and grades upward into reworked lake deposits and lagoon fill about 1.5 m thick in which a calcic paleosol is developed. The paleosol is overlain by well sorted sand and gravel (unit 3?) of a younger lake cycle.

Ostracodes from the marl (fig. 16) suggest that the lake in which unit 2 was deposited may have reached a level no higher than levels equivalent to the Stansbury shoreline of Lake Bonneville. Only two species of ostracode are present in the unit-2 samples, *Limnocythere staplini*, and *Candona caudata* (?), and the assemblage is dominated by *L. staplini*. By comparison, this assemblage is found in the lower part of the Lake Bonneville marl, which was deposited before the lake reached the Stansbury shoreline. At lake levels higher than the Stansbury, the water chemistry changed, and other ostracodes begin to replace *L. staplini* (e.g., *L. ceriotuberosa*) (Forester, 1987; Thompson et al., 1990; Oviatt, unpublished data). Note that reconstructions of the Cutler Dam Lake cycle (~40–70 ka; fig. 2; Oviatt et al., 1987) suggest that it reached a elevation of no higher than about 4400 ft (1340 m), which is roughly the elevation of the low point of the Stansbury oscillation of Lake Bonneville. The highest level attained during the Little Valley Lake cycle (~150 ka) was an elevation between the Bonneville and Provo shorelines (of Lake Bonneville), and ostracode assemblages from marl of Little Valley age are more diverse (Oviatt, unpublished data). Therefore, the ostracodes in the unit-2 marl suggest that unit 2 was deposited in a relatively low pre-Bonneville lake, possibly of Cutler Dam age.

The lagoon sediments in which the paleosol is developed, and which overlie the unit-2 marl, can be traced to the west across the floor of the pit, where they grade into silty lagoon fill that contains a white bed, 30–50 cm thick, of reworked fine-grained volcanic ash. Microprobe analyses of a sample of the ash suggest a correlation with one of the Mt. St. Helens ashes, which have been dated between ~40 ka and 150 ka (Mike Perkins, and Andrei Sarna-Wojcicki, personal communication, 1996). The possible correlates are a Mt. St. Helens C tephra, with a probable age between 40 and 50 ka, and another tephra from a core from Carp Lake, OR, with an age estimated between 75 and 125 ka.

Table 1 shows the results of amino acid analyses of ostracodes from the Lakeside unit-2 marl compared with results from deposits of known age in the Bonneville basin and elsewhere (analyses and data by Darrell Kaufman, Utah State University). The ostracode amino-acid data suggest a marl age older than Lake Bonneville (which is also clearly indicated by the overlying paleosol), and younger than the Little Valley lake cycle (about 150 ka; Scott et al., 1983). The amino acid ratios are similar to those for ostracodes from deposits of the Cutler Dam Alloformation, which was deposited sometime between 40 and 70 ka (figure 2; Oviatt et al., 1987). If the correlation with the Cutler Dam Alloformation is correct, the overlying paleosol is probably correlative with the Fielding Geosol (Oviatt et al., 1987). Further refinements to the basin-wide chronology of the Cutler Dam lake cycle, and tests of the hypothesis that unit 2 in the Lakeside gravel pit is Cutler Dam in age, are needed.

Units 3 and 4 are gravels that overlie unit 2 in the east wall of the pit, and also thicken to the south into foreset gravel. Each of the gravel units in the east wall, except unit 3, has a boulder or cobble lag at its top, which was probably deposited by waves during the regressive phase of that lake cycle or during the transgressive phase of the succeeding lake cycle. A thin (~10 cm) fine-grained unit between units 3 and 2 may be composed of eolian silt. Units 3 and 4 have not been dated and nothing is known about the sizes of the lakes in which they were deposited.

Bonneville deposits (unit 5) at the top of the sequence also consist of horizontally bedded gravel in the east wall, but can be traced to the south into foreset gravel of a barrier beach. Although the gravel barrier has not been dated directly, it is near the right elevation (4300 ft; 1310 m) to be possibly equivalent to the transgressive-phase Pilot Valley shoreline. Most of the gravel barrier has been removed, but the Bonneville marl on the back (lagoon) side of the barrier is well exposed.

Ostracodes from the Bonneville marl in the Lakeside gravel pit permit correlations with typical white marl sections elsewhere in the Bonneville basin, and demonstrate that although the marl on the barrier is thin and sandy, it has some similarities with other marl sections. For instance, the ostracodes at the base of the section consist primarily of *Limnocythere staplini*, which is typical of pre-Stansbury marl (~~25–~~22 ka), and the ostracodes near the top of the section are typical of deep-water phases of Lake Bonneville (fig. 4). A thin carbonate crust about halfway up in the marl may represent the abrupt contact at the base of the Bonneville flood bed, and would therefore date to approximately 14.5 ka. However the crust probably formed long after deposition of the section; secondary carbonate precipitated at the contact between the less permeable sediments below, and the sandier, finely bedded marl above. We observed a similar carbonate crust at the Bonneville Flood contact at the Puddle Valley gravel pit. At the Lakeside gravel pit, however, the carbonate crust marks a level in the marl between deposits of approximately Stansbury age and deposits of Provo age, as determined from the ostracodes. Therefore, it appears that the massive marl deposited during the deepest-water phase of Lake Bonneville is missing from this section.

Return to gravel road, reset mileage to zero, and turn north.

0.3 Lakeside–Turn left along base of hill. Pass large quarry on left.

0.7 Turn right and cross railroad tracks.

0.8 Turn left parallel to railroad tracks. This road is *private property* and its use must be cleared with Southern Pacific Railroad.

11.7 Pump station and canal. This system was built in 1986 to pump flood water from Great Salt Lake westard to the Great Salt Lake Desert, where it would increase evaporation. The plan was successful in that it helped lower the lake faster than it would have on its own. Reduced precipitation and increased evaporation, starting in 1987, further ensured the lake's decline to less destructive levels. Excellent exposures along the canal walls illustrate Holocene, Lake Bonneville, and pre-Bonneville deposits, as well as Miocene and Paleozoic strata and the faults affecting those older strata.

*Figure 16. Photo of older marl (unit-2 marl) at Lakeside gravel pit. Ostracode samples are lettered (**D** = Ls, **C** = Ls, **B** = Cc, Ls, **A** = Ls, Cc). See figure 4 for explanation of abbreviations.*

13.9 Bear right on dirt road.

14.1 Make acute right turn toward the north. BLM sign on the road reads: "Kelton 41 mi."

15.1 Stop along road where quarry edge on left is cut by gully.

STOP 4. Pilot Valley shoreline.

This long (6.2 km) narrow quarry, which was developed by the railroad in the early part of the 20th century to build the Lucin cutoff, beautifully displays a series of beach ridges that extend along the south flank of the Hogup Mountains (fig. 17). The beach gravels lie on loess and alluvium in which a paleosol is developed (exposed in three places in the west half of the quarry) and are overlain by Bonneville marl, and therefore are early transgressive Bonneville features. They represent the earliest regionally correlatable beaches of Lake Bonneville, informally termed the Pilot Valley shoreline by Miller (1990). Here and elsewhere, the shoreline is marked by a set of two to four beaches that climb from about 4275 to 4295 ft in altitude, with maximum development typically at 4285 ft.

Here we examine some gully exposures on the back (lagoon) side of a barrier where the white marl lies on beach

Table 1. Amino acid ratios for ostracodes (Candona *and* Limnocythere) *from deposits of various ages. Analyses and data provided by Darrell Kaufman, Utah State University.*

Lab No.*	Lake Cycle (age, ka)	Locality	Asp†	Glu†	Ala†	Ile†
Candona results:						
2030	post-Provo (12)	Fielding	0.196 ± 0.017 (2)	0.048 ± 0.007	0.075 ± 0.013	0.034 ± 0.012
2047	Bonneville (19)	Black Rock	0.275 ± 0.008 (10)	0.086 ± 0.005	0.172 ± 0.008	0.075 ± 0.008
2046	Bonneville (21)	Little Valley	0.300 ± 0.010 (10)	0.080 ± 0.007	0.184 ± 0.013	0.091 ± 0.015
2042	Bonneville (~25)	West Gully	0.299 ± 0.011 (9)	0.082 ± 0.009	0.194 ± 0.023	0.095 ± 0.014
2096	Bonneville (?)	Bear River	0.237 ± 0.005 (5)	0.062 ± 0.009	0.147 ± 0.005	0.075 ± 0.011
2041	Cutler Dam (~40?–70?)	West Gully	0.308 ± 0.025 (2)	0.125 ± —	0.361 ± 0.037	0.114 ± —
2095	Cutler Dam (~40?–70?)	Bear River	0.292 ± 0.015 (6)	0.079 ± 0.009	0.230 ± 0.029	0.099 ± 0.019
2036	unit-2 marl (age ?)	Lakeside	0.325 ± 0.038 (4)	0.106 ± 0.025	0.284 ± 0.062	0.096 ± 0.054
2032	— (~70)	Anna River, OR	0.304 ± 0.013 (9)	0.124 ± 0.017	0.223 ± 0.036	0.096 ± 0.014
2043	Little Valley (~150)	West Gully	0.481 ± 0.030 (8)	0.175 ± 0.015	0.424 ± 0.033	0.184 ± 0.039
2037	Little Valley (~150)	Little Valley	0.417 ± 0.010 (7)	0.194 ± 0.013	0.478 ± 0.021	0.233 ± 0.041
2056	— (~150 ka)	Anna River, OR	0.374 ± 0.012 (9)	0.160 ± 0.010	0.392 ± 0.024	0.271 ± 0.086
Limnocythere results:						
2103	Bonneville (~25)	West Gully	0.242 ± 0.006 (6)	0.043 ± 0.002	0.127 ± 0.002	0.024 ± 0.002
2101	Cutler Dam (~40?–70?)	West Gully	0.223 ± 0.012 (5)	0.066 ± 0.005	0.192 ± 0.013	0.026 ± 0.003
2148/49	unit-2 marl (age ?)	Lakeside	0.296 ± 0.040 (10)	0.092 ± 0.092	0.247 ± 0.070	0.037 ± 0.013
2102	Little Valley (~150)	West Gully	0.325 ± 0.015 (5)	0.103 ± 0.007	0.288 ± 0.010	0.061 ± 0.007
2107/50	Little Valley (~150)	Little Valley	0.359 ± 0.021 (10)	0.139 ± 0.019	0.388 ± 0.031	0.132 ± 0.039

*All samples were analyzed by Darrell Kaufman at the Amino Acid Geochronology Laboratory at Utah State University; therefore, each lab number has the prefix UAL-, e g., UAL-2042. The samples were analyzed using a new reverse-phase HPLC procedure which is presented in Kaufman and Manley (in review)

†DL ratios and standard deviations for aspartic acid (Asp), glutamic acid (Glu), and alanine (Ala), the ratio value for isoleucine (Ile) is D-alloisoleucine L-isoleucine (aIle/Ile). Numbers in parentheses indicate number of separate subsamples prepared from each sample. Each subsample was composed of 0.1–0 2 mg of ostracodes (10–40 individuals)

gravel. The marl represents most of the Bonneville lake history, as confirmed by stratigraphy and ostracode study (fig. 17). The marl is about 6 ft (2 m) thick, and overlies gravel and coarse oolitic sand of the barrier complex (fig. 17). Ostracodes from the marl permit correlations with other marl sections in the Bonneville basin. An abrupt contact overlain by sandy marl probably represents the Bonneville flood contact (based on its field appearance and the ostracode faunas).

Internal unconformities within the barrier-beach gravels may owe to overlapping beach development here. Figure 18 shows two well-developed beach ridges; stop 4 is in the lower one, which clearly predates the white marl. Stratigraphic relationships for the upper beach ridge are unclear (that is, exposures do not indicate whether the marl overlies it or underlies it), so it could be either a Pilot Valley, or Gilbert beach.

These gravel beaches are the earliest widely developed beaches recognized for Lake Bonneville, and have been tracked across the northern Bonneville basin from Pilot Valley to the Rozel Hills (fig. 19). If they can be identified in other parts of the basin, they can serve as an important leveling marker because they formed so early in Lake Bonneville's history that little isostatic deflection should have taken place before their development.

Reset mileage to zero and continue on gravel road to the northwest.

0.9 Climb to crest of uppermost gravel beach of the Pilot Valley shoreline in this location; altitude is between 4285 and 4290 ft.

8.1 Cross Provo shoreline, expressed as two barrier beaches.

9.3 Cross tombolos below the Bonneville shoreline. The Bonneville is visible to the east and west of the tombolo. Tremendous Bonneville and Provo spits are visible to the north along the skyline.

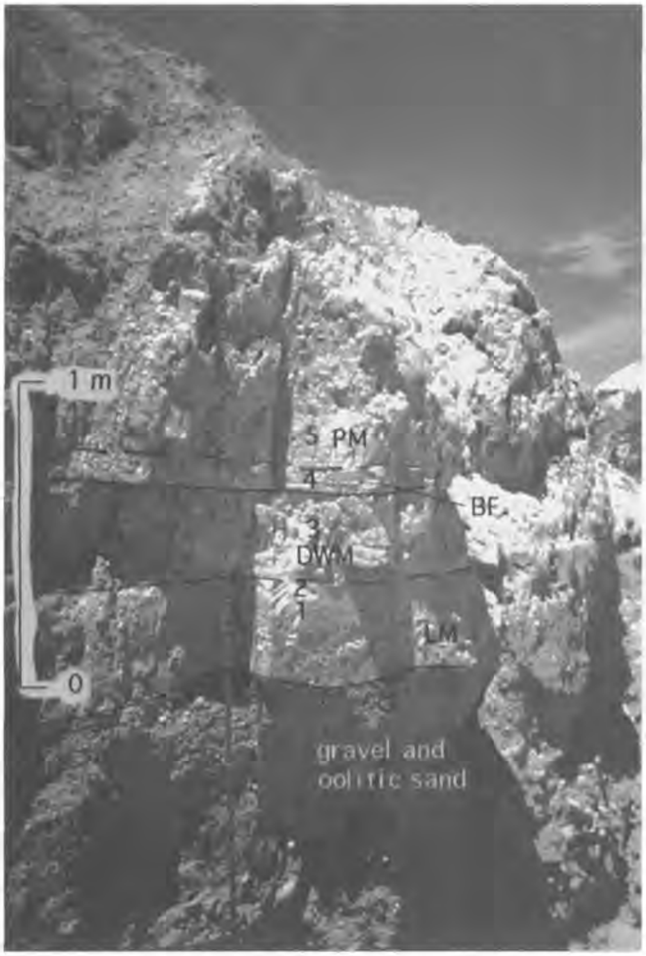

*Figure 17. Photo of marl section at stop 4 (Pilot Valley shoreline). LM = laminated (transgressive) marl; DWM = deep-water marl; BF = Bonneville flood bed; PM = Provo marl. Ostracode samples are numbered (**5** = Ca, Lc, **4** = Lc, Cc, Cd, Ca/c, **3** = Lc, Cc, **2** = Cc, Lc, Ls, **1** = Cc, Lc, Ls). See figure 4 for explanation of abbreviations.*

Figure 18. Area of Stop 4 shown on aerial photograph taken October 21, 1969. Small white arrows point to major gravel beaches. Linear gravel pit climbs northwestward from lower to upper beach. Area represented by photo is approximately 3.8 km wide.

These form the upper part of a feature called the Fingerpoint, which we will cross after STOP 5.

9.4 Bear right at intersection.

9.6 Turn right on road to the Fingerpoint and Kelton.

10.3 Cross Provo shoreline.

15.5 Park on right side of road after dropping down off the Gilbert beach. Walk southeast to the breach in the barrier beach.

STOP 5. Stratigraphy at the Gilbert shoreline (at the Fingerpoint).

The exposure at stop 5 is a good contrast to the sequence at the Pilot Valley shoreline stop (stop 4). At stop 5, the white marl, which consists of a typical lithologic and ostracode sequence, is overlain by gravel of a barrier beach indicating that the beach is regressive. The beach is interpreted as a local segment of the Gilbert shoreline because it has an appropriate elevation (4271 ft) and relative age (post-Bonneville). Gravel beneath the white marl at the Fingerpoint stop is transgressive in age and approximately the same age as the Pilot Valley shoreline.

The white marl at this stop is somewhat different in appearance from the marl at other locations because it was deposited in a site that had considerable wave energy. Consequently the section overall is relatively sandy, and there are clean sand beds interspersed with the marl (figs. 20 and 21). We interpret the sand beds as turbidites, possibly generated by slumps off the large spits of the Fingerpoint at higher elevations. Nevertheless, the ostracode sequence is easily correlated with that of other Bonneville sections (fig. 4).

Data on the total carbonate, carbonate mineralogy, and sand content of a short core collected at the outcrop are presented in fig. 21. Note the abrupt increase in aragonite above the Bonneville Flood contact. Also note that the

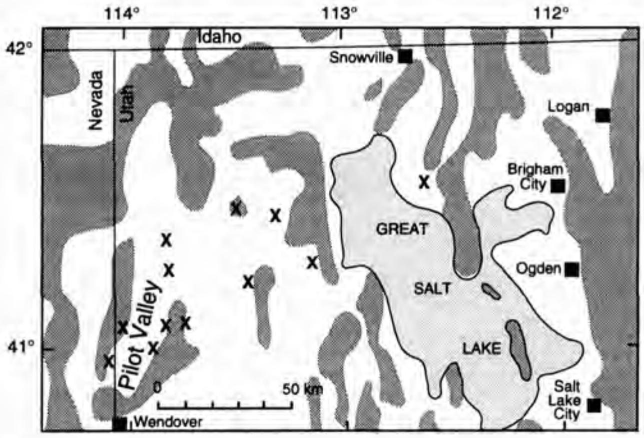

Figure 19. Map showing known localities of the Pilot Valley shoreline in NW Utah.

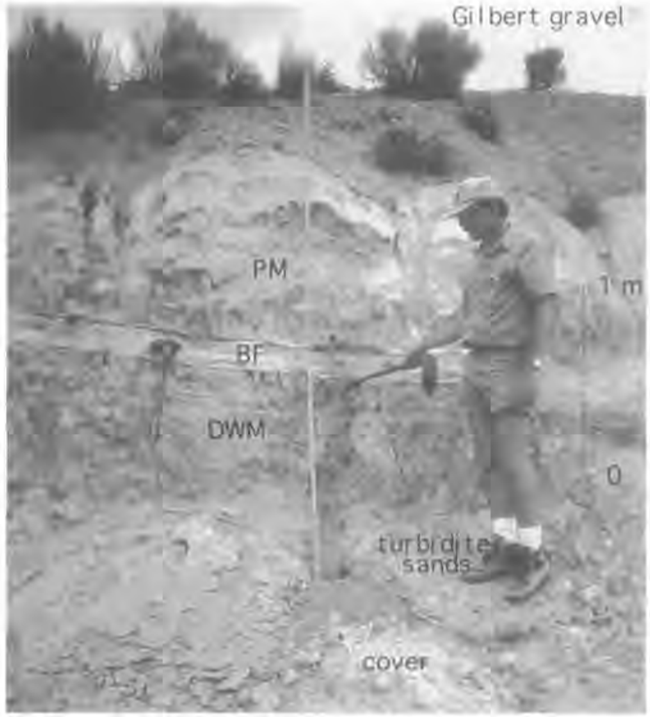

Figure 20. Photo of marl section at stop 5 (the Fingerpoint). DWM = deep-water marl; BF = Bonneville flood bed; PM = Provo marl. The marl section is underlain by transgressive Bonneville gravel, and overlain by regressive gravel of the Gilbert shoreline.

aragonite curve peaks after the total carbonate curve peaks. Similar trends have been noted in other white marl cores, including those described by Spencer et al., (1984) from the Great Salt Lake, who interpreted the rise in aragonite as having been caused by the increase in Mg/Ca ratio—Ca was quickly used up in the precipitation of carbonates as the lake evaporated to lower and lower levels at the end of the Bonneville regression.

Reset mileage to zero. We will drive to Utah Route 30 and then to Tremonton for the end of Day 1. Continue northeast on gravel road.

0.6 Crest of the Fingerpoint. Continue north toward Kelton. The Fingerpoint is a 9.5-mile long feature extending south from the Hogup Mountains as a series of platforms and beach ridges that represent every major shoreline of Lake Bonneville and many more local shorelines (fig. 22). Looking upslope along the Fingerpoint, several huge gravel prominences mark spits and V-shaped barrier beaches that can be found by driving in that direction. Downslope, the Fingerpoint extends southward to end in several recurved beaches, the lowest of which is the sand and gravel beach that formed during 1986–1987. Although some bedrock control for this enormous feature probably existed, the Fingerpoint is composed entirely of gravel in surface exposures. This is one of the more impressive examples of enormous volumes of gravel transported by Lake Bonneville and its predecessors.

1.0 Bear right at fork in road.

3.1 Dolphin Island to the east is surrounded by mud flats. The high part of this island is composed of beachrock composed of cemented angular clasts of the Oquirrh Formation. Tails of lacustrine and eolian oolitic sand extend southward from the island.

16.6 Climb across a Gilbert barrier beach and across a large double tombolo connecting the mainland (Hogup Mountains) to an island (Crocodile Mountain).

23.2 The basalt-capped butte on the left is Table Mountain. The basalt is probably Pliocene (Miller et al., 1995).

24.2 Bear right (east) at the intersection.

26.8 Continue straight through crossroads. Kelton cemetery is on the right.

26.9 Townsite of Kelton. Bear left. Kelton was a major railroad depot on the original transcontinental railroad across the Great Salt Lake basin before the Lucin cutoff was built in 1904.

27.1 Continue straight at road junction. Follow signs to State Rte. 30.

30.1 Route 30. Turn right to Curlew Junction, turn right at Curlew Junction, and follow Rte. 30 to I-84 (16 miles). Follow I-84 east to Tremonton.

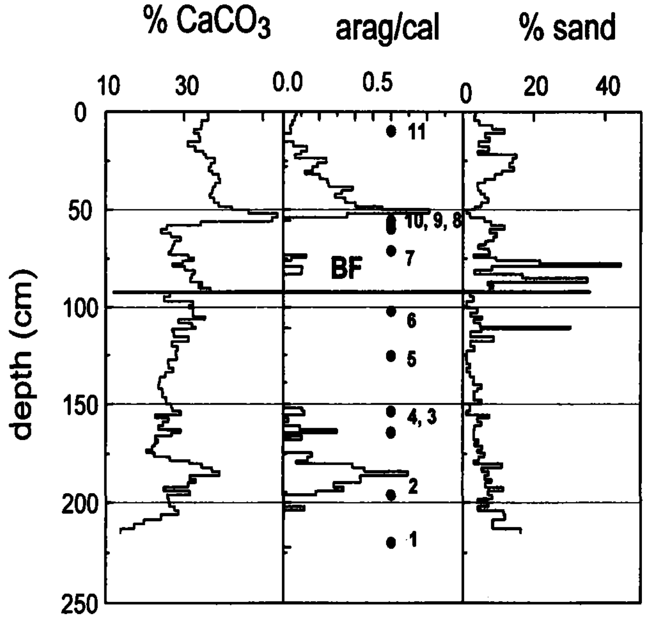

Figure 21. Lab data for a core through the marl section at stop 5. BF marks the base of the Bonneville flood bed in the core. Ostracode samples are numbered (11 = Lc, C. sp., 10 = Ca?, Lc, 9 = Ca, Cc, Lc, Cyl, 8 = Ca, Lc, Cyl, 7 = Ca, Cc, Lc, 6 = Lc, Ca?, 5 = Ca, Lc, 4 = Lc, Cc, Ca, Ls, 3 = Lc, C. sp., 2 = Lc, Cc, Ls, 1 = Cc, Ls). See figure 4 for explanation of abbreviations.

DAY 2

Travel west from Tremonton on I-84. We will cross several basins and ranges on the freeway, and then return eastward at lower altitudes nearer to Great Salt Lake.

Mile 37. Exposures of Lake Bonneville gravel in the large quarry pits on the north side of the freeway display the bewildering complexity of the beach gravels, including strongly cemented beds, and a variety of foresets and backsets. This gravel is probably mostly of Stansbury age.

Mile 34. Cross Provo shoreline as we climb the Blue Springs Hills. A barn is on the Provo platform on the north side of the freeway.

Mile 26. Cross Provo shoreline as we descend into Blue Creek Valley.

Mile 22. Cross Provo shoreline where it forms an extensive platform of sand and gravel in central Blue Creek Valley. Exposures near here, where Blue Creek gullied across the Provo barrier, display outstanding examples of rhythmically bedded near-shore sands, old alluvial units and paleosols, and a thick section of older (Little Valley lake cycle) marl.

Mile 18.3. Cross Bonneville shoreline.

Mile 17. Rattlesnake Pass. Black basalt K-Ar dated at 13.0 ± 0.3 Ma (unpublished USGS data) is exposed in the roadcuts. Ahead about 1.5 miles, another roadcut exposes the same basalt flows. There, loess deposits lying on the basalt apparently are those that yielded middle Pleistocene rodent fossils (C.A Repenning, oral communication., 1989). The loess contains several strongly developed calcic soil horizons. Normal faults at the west side of the roadcut displace basalt down to the west, and also cut a different (younger?) loess with less soil development.

Mile 16. A fault is well exposed on the north side of the freeway in the road cut. The fault places Miocene basalt against the late Paleozoic Oquirrh Formation.

Mile 13. Cross Bonneville shoreline.

Mile 9. Cross Provo shoreline as we descend into Curlew Valley.

Mile 5. Take exit and turn left (west) across the freeway. Set mileage to zero on overpass.

0.5	Turn left on small gravel road and through metal gate. (Permission required at Rose Ranch).
0.8	Proceed through corral.
0.9	Stop next to cut bank of gully on right. Walk about 100 ft west to a place to descend the bank to the gully floor, and east along the base of the wall to study the Lake Bonneville section.

STOP 6. Rose Ranch Section.

Exposures directly downstream from Rose Ranch Reservoir expose a complete Bonneville stratigraphic section at an elevation (4505 ft; 1373 m) close to the Stansbury shoreline. We will examine a section exposed near the north abutment of the dam where the base of the Bonneville section is not exposed. The base of the section can be seen by walking south across the dam to the south bank of Deep Creek, where a strongly developed calcic horizon, developed in loess, is exposed beneath the Bonneville sequence.

Ripple-laminated to massive fine sand at the base of the Bonneville section (fig. 23) is overlain by about 0.75 m of brown, blocky mud with oxidized root holes, probably deposited in deltaic or marsh environments in the estuary of Deep Creek as Lake Bonneville began to rise at the end of the Stansbury oscillation about 20 ka. The blocky mud is overlain by 1.4–0.75 m of laminated sandy marl, then 2.8–1.4 m of pink massive marl. A finely bedded sandy marl unit about 12 cm thick in the upper third of the massive marl may represent deposition during a fluctuation during the transgressive phase higher than the Stansbury shoreline (such as U1, fig. 5). An abrupt contact at the top of the massive marl is marked by pebbles and sand and overlain by white marl about 1.2 m thick. The modern soil is developed in this unit. We interpret the abrupt contact as the Bonneville flood contact based on its abruptness and on the appearance of the ostracode *Cytherissa lacustris* in the marl above it (fig. 4).

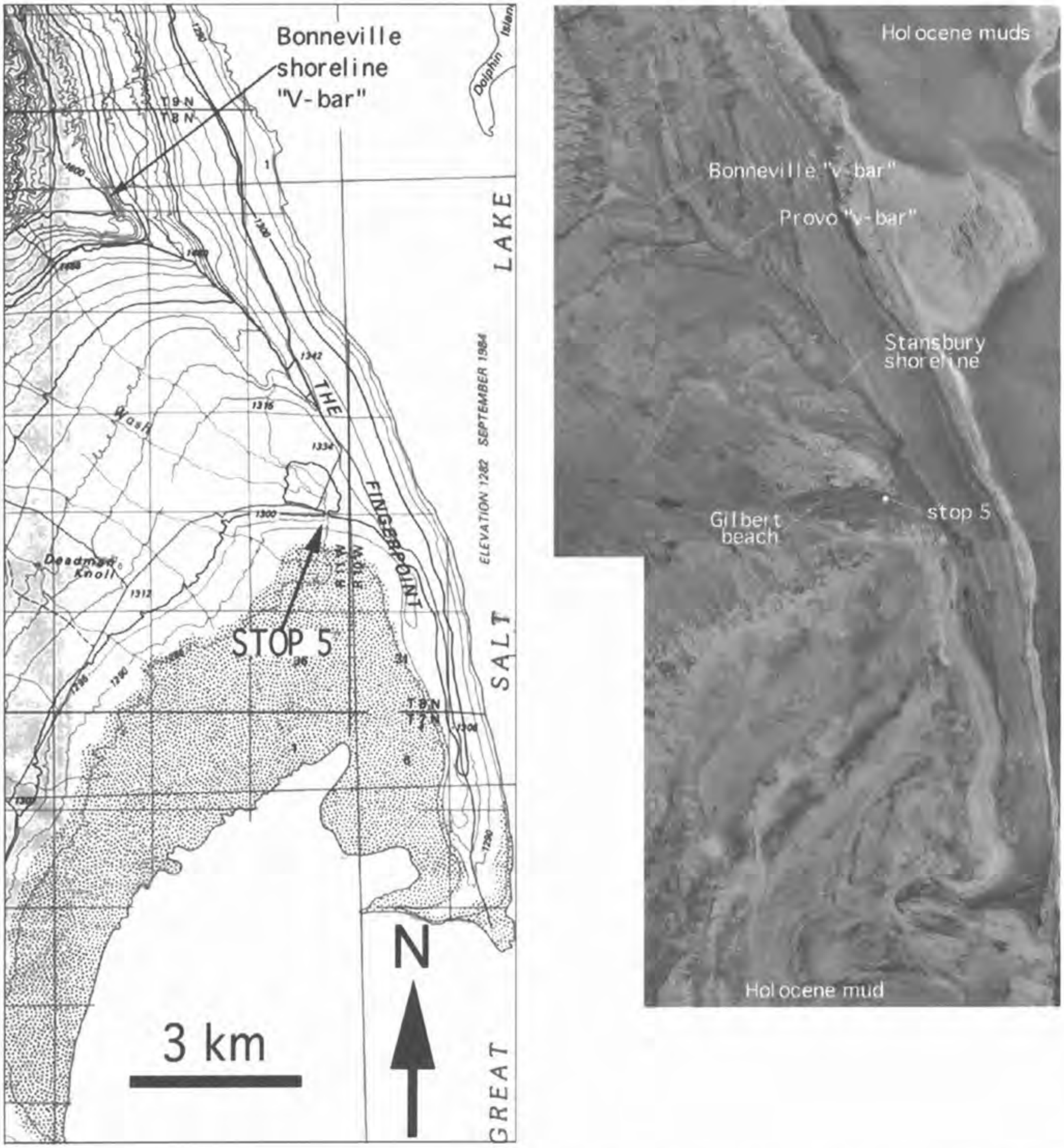

Figure 22. Map and aerial photographs of the Fingerpoint, showing roads and shorelines. Aerial photographs taken June 22, 1953. Map from U.S. Geological Survey 1:100,000-scale Newfoundland Mountains quadrangle, 1988. Contours in meters, interval 20 meters.

*Figure 23. Photo of Rose Ranch marl section at stop 6. BBM = brown, blocky mud; LM = laminated (transgressive) marl; DWM = deep-water marl; BF(?) = possible Bonneville flood bed; PM(?) = possible Provo marl. Numbered ostracode samples (**8** = Cc, Lc, Ce?, **7** = Cyl, Cc/a, Cc, Lc, **6** = Lc, Ca, Cyl, **5** = Lc, Lsa, Cc/a, Ls, **4** = Ca, Lc, Cc, **3B** = Ca, Lc, Cc, Ce?, **3A** = Ca, Lc, Cc, Ce?, **2** = Ls, Cc, **1** = Cr, Ls). See figure 4 for explanation of abbreviations.*

Here, and elsewhere in Curlew Valley, much of the marl section is preserved and locally exposed in gullies (Miller and Langrock, 1997a), an unusual occurrence in the Bonneville basin. A combination of factors probably led to this situation: (1) Deep Creek fed fine clastic material to the lake that led to fairly thick marl accumulations. (2) The low-gradient valley was not extensively eroded following lake withdrawal. (3) Deep Creek deeply entrenched the marl plains, and did not deposit appreciable sediment on the marl.

Return to vehicles and retrace route to I-84; enter freeway headed east.

Mile 7. Snowville exit. Exit the freeway and set mileage to zero at stop sign. Turn right (south) on paved road, then immediate right onto gravel road. Continue on main gravel road.

6.3 Proceed south past road to left.

9.6 View of Cedar Hill, a shield volcano about 1.2 million years old, on the west (Miller and Langrock, 1997b). On the east is Johnson Hill, etched by a prominent Provo shoreline. Johnson Hill lies between Curlew Valley and Sage Valley, a small internally-drained valley. Sage Valley drained abruptly, creating a small sand blanket projecting into Curlew Valley. Erosion caused by the rapid draining, apparently during the rapid regression from the Provo shoreline, truncated several shorelines.

13.2 Park on the barrier beach and look at the quarry on the west side of the road.

STOP 7. Stansbury shoreline and Quaternary volcanoes.

Barrier beach deposits form a prominent shoreline here and mark the upper Stansbury shorezone. A benchmark on the east side of the road on the beach crest is 4497 ft (1370 m). Structure within the barrier beach can be examined in the quarry walls on the west side of the road.

From at least 1.2 million years to 440,000 years ago basalt erupted intermittently to form the three shields along Curlew Valley just west of us, from Cedar Hill on the north to Locomotive Springs well to the south (fig. 24) (Miller and Langrock, 1997b). In addition, basaltic ash (the Hansel Valley ash) was erupted from an uncertain location west of Hansel Valley and probably in Curlew Valley, on the basis of chemical similarity with Curlew basalts and the location of the ejecta blanket (Miller et al., 1995). K-Ar ages for the shields are 1.16 ± 0.08, 0.72 ± 0.15, and 0.44 ± 0.10 Ma from north to south (Miller et al., 1995). The two northern shields retain summit collapse features, and individual flows can be traced down the flanks. The southern shield is small and may have been eroded more by waves of pluvial lakes; it shows only a flat summit that may once have been a crater. The Quaternary shield volcanoes of eastern Curlew Valley are similar in mineralogy and geochemistry but decrease systematically in age southward toward the Great Salt Lake, suggesting a progressive movement of an eruptive center with time, at a rate of about 2.1 cm/year. The recurrence of eruptions in this system is not well determined, but the volcanoes seem to have formed every 300,000 to 400,000 years. If the Hansel Valley ash is considered to be a minor event, the next large eruption is possible at any time (Miller et al., 1995) and may be located in Great Salt Lake. Such an eruption could severely impact the Wasatch Front population.

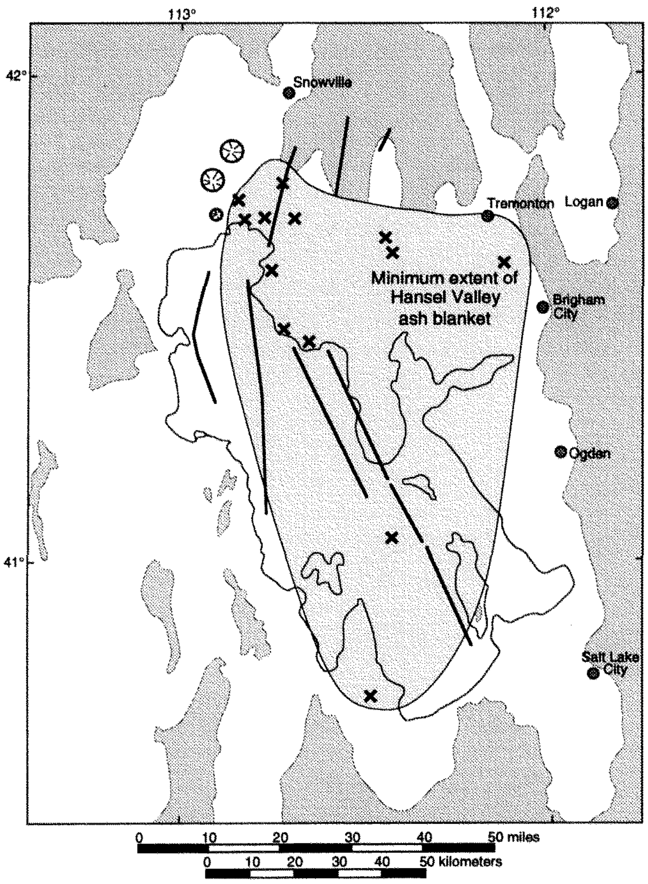

Figure 24. Selected volcanic features and faults of the Great Salt Lake area. X, Hansel Valley ash location. Volcanoes in Curlew Valley shown by circles with radiating lines. Faults shown are all Holocene.

The Hansel Valley ash has been identified in one exposure in eastern Curlew Valley and in roughly a dozen exposures to the east and southeast in Hansel and Blue Creek Valleys, the Rozel Hills, and at the Bear River (figs. 9 and 24). It also has been identified in cores from the south arm of Great Salt Lake (Spencer et al., 1984; Oviatt and Nash, 1989), and the Burmester core at the south margin of the lake. The explosive eruption that distributed the Hansel Valley ash likely was caused by interaction of magma with water in the near surface or at the surface. A source within water-charged lowlands of Curlew Valley or within Lake Bonneville is likely, but we have not yet discovered a tephra ring, coarse proximal deposits, or other indicators of the eruptive vent despite extensive field work. It is possible that the Hansel Valley ash eruption was triggered by the load of Lake Bonneville; several basaltic volcanoes in the Sevier Desert erupted into Lake Bonneville (Oviatt and Nash, 1989).

Reset mileage and proceed south on gravel road.

1.4 The shield volcano on the west is about 720 ka.

2.4 The low basalt hill to the east of the road is blanketed by Bonneville marl. The Hansel Valley ash is at the base of the marl.

5.0 Cross Gilbert shoreline. It is a low spit on the west that increases in prominence eastward toward Monument Point.

6.1 Turn left on gravel road just north of the old railroad grade. Locomotive Springs shield volcano (~440 ka) lies to the south (Miller and Langrock, 1997c).

8.2 Proceed across a Holocene Great Salt Lake barrier beach at about 4240 ft altitude. It postdates the Gilbert shoreline, but is otherwise undated.

10.3 Proceed past Monument Point (see Miller and Langrock, 1997d). By driving south toward Lone Rock, a good section of marl, including the Hansel Valley ash at the base, can be examined along wave-cut bluffs formed by Great Salt Lake during the highstands of 1986 and 1987.

14.1 Bear left at fork.

15.2 Climb onto Gilbert barrier beach from Gilbert erosional notch.

16.1 Gilbert barrier beach visible to south of road. Its crest is slightly above 4260 ft. To the east, it merges with the level of the road.

17.0 Stop on road.

STOP 8. Faulted Gilbert spit.

This stop is at a degraded scarp created by the 1934 Hansel Valley earthquake and previous faulting events. The Hansel Valley fault has displaced the surface of the Gilbert spit down to the east. The fault strikes slightly east of north, and its scarp is visible north of the road for some distance. In the mud flats south of the road, the mud was cracked and mud volcanoes formed in 1934, but only scattered evidence for the location of the fault can be seen now. The 1934 Hansel Valley earthquake is the only historic ground-rupturing seismic event in northern Utah, despite the highly active seismicity of this region (Christenson et al., 1987). Historic felt earthquakes include the magnitude 6 and larger events in Hansel Valley during 1909 and 1934 (Arabasz et al., 1994). Frequent smaller-magnitude earthquakes ($M<4$) occur in broader zones in the area, including Blue Creek, Hansel, and Curlew Valleys, and northern Great Salt Lake and the Rozel Hills (Christenson et al., 1987).

The March 1934 magnitude 6.6 earthquake in Hansel Valley (Christenson et al., 1987) produced surface rupture along four zones, of which the zone where we stopped had as much as 20 inches of down-to-the-east offset. Some of the faults, including this one, show evidence for earlier displacements (Robison and McCalpin, 1987). The earthquake caused severe damage in local towns and ranches, and it even caused damage in cities along the Wasatch Front. The evidence for repeat faulting at this location makes it clear that a threat for future earthquakes is real, but the pattern of recurrence is complex and not easily converted as a predictive tool. The recurrence interval *appears* to be several thousands of years.

Significant subsidence was noted by two types of studies following the 1934 earthquake. Adams (1938) compared by triangulation the nearby shoreline of Great Salt Lake in November 1934 to the shorelines surveyed by Captain Stansbury in 1850. Despite the lake being 6 feet lower in 1934 than in 1850, the shorelines overlapped. Adams concluded that about 4 feet of general subsidence of southern Hansel Valley took place between 1850 and 1934, with subsidence locally as great as 6 feet. Complications caused by causeways and dikes constructed after 1850 were not accounted for, but Adams showed that soundings and shorelines indicated little subsidence farther south in the lake. Adams (1938) also described the results of re-leveling the railroad grade across the mouth of Hansel Valley. Comparing 1911 and 1934 surveys, ground subsidence was 1.2 feet in lower Hansel Valley and could be identified to the west for 10 miles into Curlew Valley at diminished magnitude. These data suggest that only about one quarter of the 84-year subsidence record was produced during the Hansel Valley earthquake of 1934. A 1953 railroad levelling showed regional *uplift* of this same area west from the Hansel Valley fault (Bucknam, 1979).

Another potentially profitable approach for examining the neotectonic record would be to carefully level lakeshore features, such as the Gilbert spits, beaches, and abrasion platforms. Such a study could identify long-term subsidence and uplift relative to regionally established elevations for these features. A reconnaissance analysis of topographic data suggests that the west side of this fault is upthrown; elevations for the Gilbert spit and the 4240-ft shoreline to the east of the fault are consistent with regional values. Significant subsidence to the south, identified by comparing Great Salt Lake shorelines, may be a related but different manifestation of local tectonics. Careful study of shorelines since aerial photographs and satellite surveys began could address this problem over a time-span of several decades.

The Gilbert spit begins at about this location and extends to the east about two km. Wave energy from the southwest carried gravel northeast during the Gilbert lake's highstand to create this spit. As we drive east along the spit note the rapid drops of the surface to lower altitudes as we approach its terminus; these lower-altitude spits formed during regression from the Gilbert highstand or as other lake rises built onto the Gilbert spit. The 4240-ft shoreline is constructed along the front of the Gilbert spit in many places, and forms much of the end of the spit.

Reset mileage to zero and continue east.

2.4 Bear left at intersection. Elevation of the spit surface is 4242 ft here.

3.6 Stop along main road next to obscure road on right in greasewood plain. Take care not to drive in the greasewood; it destroys tires! Walk about 1 mile along this obscure road and continue into Hansel Valley Wash as road ends. The first half mile of the wash has been modified by bulldozer, but eventually the wash turns to its original northeasterly orientation. Proceed up this original wash several hundred feet until the marl section is about 3 m thick as exposed in walls on the east side of the gully.

STOP 9. Hansel Valley Wash.

This marl section is notable for several features, including: (1) its lateral continuity for several km along Hansel Valley, (2) presence of the Hansel Valley ash near the base, and (3) soft-sediment disruption of the marl, possibly induced by seismicity.

The Bonneville section at this stop is fairly complete because it was deposited on a low gradient valley floor at a relatively low elevation (4330 ft; 1320 m). Here we can observe the sequence of facies changes in the marl that can be see at many similar sections around the basin. Coarse-grained deposits at the base of the section are interpreted as marking the initial transgression of Lake Bonneville (fig. 25). The coarse sand grades upward into blocky mud that contains oxidized root holes; we interpret this unit as having been deposited in a marsh or lagoon environment at the margin of the transgressing lake. Overlying the transgressive deposits is a sequence of laminated marl 3.2 ft (0.98 m) thick (early-transgressive and Stansbury), which grades upward into more massive, greenish gray to pink marl about 4 ft (1.3 m) thick (deep-water marl). The upper contact of the massive marl is abrupt and the overlying bed of ripple-laminated sand and sandy marl is about 0.4 ft (12 cm) thick (the Bonneville flood bed). Its upper contact is gradational into another massive marl (Provo marl), which coarsens upward and is disrupted in its upper part by modern soil development. Ostracodes and diatoms (fig. 25) support the interpretation of this sequence as a cycle, representing the transgression, deep water, and regression of Lake Bonneville.

One thing to speculate on at this section is the origin of the ripple-laminated beds in the Bonneville flood bed (the 12 cm thick bed between the two massive marls). Our interpretation is that during and immediately after the Bonneville flood, when lake level dropped catastrophically

Figure 25. Photo of Hansel Valley Wash marl section (stop 9). T = transgressive mud and sand; LM = laminated (transgressive) marl; DWM = deep-water marl; BF = Bonneville flood bed; PM = Provo marl. Lettered ostracode and diatom samples. Ostracode samples: ***W*** *= Cyl, Ce, Ca, Lc, Lsa,* ***V*** *= Ce, Cc, Ca, Lc,* ***U*** *= Cc, Ce, Ca, LcLsa,* ***T*** *= Lc, Cc, Ca, Ce,* ***S*** *= Lc, Ls, Ca, Cc,* ***R*** *= Lc, Ca?,* ***Q*** *= Lc, Ca, Cc,* ***P*** *= Ca, Lc,* ***O*** *= Ca, Lc,* ***N*** *= Ca, Lc,* ***M*** *= Lc, Ca,* ***L*** *= Lc, C sp.,* ***K*** *= Lc, Cc, Ca, Cd,* ***J*** *= Lc, Cc, Ca, Cd,* ***I*** *= Lc, Cc,* ***H*** *= Lc, Cc, Ls,* ***G*** *= Cc, Ls,* ***F*** *= Cc, Ls,* ***E*** *= Ls, Cc,* ***D*** *= Ls, C sp.,* ***C*** *= Ls,* ***B*** *= Ls,* ***A*** *= no ostracodes. See figure 4 for explanation of abbreviations. Diatoms from Hansel Valley Wash section identified by Platt Bradbury, May 27, 1992:* ***W*** *=* Cyclotella ocellata *(cold open water),* ***V*** *=* Synedra acus *(fresh open water),* S. ulna, Cyclotella ocellata, C. caspia??, Fragilaria brevistriata, F. leptostauron, ***C-G*** *=* Fragilaria brevistriata *(shallow, moderately saline water),* F. construens *v.* subsalina, Epithemia, Mastogloia, Navicula, Amphora, Surirella, Pinnularia, *others.*

by about 100 m, vast areas of fine-grained lake-bottom sediments would have been stranded above lake level between the Bonneville and Provo shorelines. That sediment would have begun washing into the lake immediately after the flood (accounting for the thick marl and clastic deposits directly below the Provo shoreline throughout the basin, which we refer to as the Provo "dump" as per Don Currey), and provided a source for slumps and landslides that would have created turbidity currents on the lake bottom. In Hansel Valley, slumping of fine-grained sediments both above and below lake level might have been enhanced by earthquake activity.

Two cm above the base of the laminated marl is a thin (1 cm) bed of brown basaltic ash, which we have named the Hansel Valley ash (Miller et al., 1995) (formerly referred to as the "Thiokol ash" by Oviatt and Nash, 1989). We have found the Hansel Valley ash at many localities in northern Utah, including in the Burmester core at the south end of Great Salt Lake (Oviatt and Thompson, unpublished). At all known localities where the Hansel Valley ash has been found, including sediment cores from Great Salt Lake (Spencer et al., 1984), the ash bed is within a few centimeters of the base of the Bonneville section. A radiocarbon age of 26.5 ka for a core sample collected near the ash (Thompson et al., 1990) is the best available age for the eruption. Exposures in West Gully in Hansel Valley suggest that Lake Bonneville was close to an elevation of 4380 ft (1335 m) at the time the Hansel Valley ash was erupted. Despite extensive field efforts, we have not yet identified the source vent of the ash, but its chemistry is similar to that of basalts in the Curlew Valley area (Miller et al., 1995).

Note the common disrupted beds containing small faults and folds below and including the Hansel Valley ash. These features may have been caused by nearby small seismic events or larger distant events. Upstream several km, convoluted beds and hummocky cross-stratification are common in the section beneath the deep-water beds that lie below the flood bed. Robison and McCalpin (1987) suggested that these features indicate several local earthquakes, some of which displaced parts of the marl section in a tributary gully to Hansel Wash (referred to as West Gully).

Return to gravel road, set milage to zero, and turn south.

0.9 Continue straight.
5.8 Pass shortcut on left.
6.5 Turn left on gravel road toward mud flat.
11.2 Double Gilbert barrier beach. Quarry pit on the right is in one of the beaches.
11.3 Continue straight. Route following the old railroad grade is to the right.
15.0 The Provo shoreline is expressed as wave-cut notches on both sides of the road.

16.4 Cross double Provo barrier beach. As in most places where the Provo shoreline is well exposed, it consists of two beaches about 10 ft different in altitude. Gilbert (1890) noted the double character of erosional segments of the Provo shoreline, but offered no explanation. Currey (Currey and Burr, 1988) has noted three or four steps in depositional Provo-shoreline segments at a number of locations around the basin, and suggests that landsliding and scour in the overflow threshold at Red Rock Pass, Idaho, complicated by ongoing isostatic rebound, controlled lake level throughout the basin during the development of the Provo shoreline. This hypothesis could be further tested by basin-wide mapping, careful geomorphic study, and surveying of the Provo shoreline.

The best available ages for the Provo shoreline suggest that it began forming after the Bonneville flood (14.5 ka), and that the lake overflowed at this level for 500 to 1000 years (Oviatt et al., 1992; Light and Kaufman, 1996). Overflow ceased and lake level began to drop rapidly between 14 and 13.5 ka.

18.4 Cross Bonneville barrier beach.

21.8 Intersection with paved road; *continue straight* on the paved road. Golden Spike National Monument, errected to commemorate the historic meeting of the transcontinental (Union and Central Pacific railroads), is to the right. We are driving along an unconformity cut into Miocene tuff during Pliocene time. Alluvial sediment on the tuff but beneath the Bonneville sediment yielded Pliocene fossils and volcanic ash (Nelson and Miller, 1990).

23.3 Transgressive-phase spits of Lake Bonneville are well exposed to the south, at the north end of the Promontory Mountains.

26.5 Junction; continue straight.

28.5 Junction with State Highway 83. Turn right toward Brigham City.

34.6 Stop on the right side of the road near exposures of red and brown sandy sediment of the marshes of Public Shooting Grounds.

STOP 10. Gilbert shoreline stratigraphy and chronology (Public Shooting Grounds).

At this stop we will briefly examine some exposures in roadcuts of sediments associated with the regression of Lake Bonneville and the transgression to the Gilbert shoreline. The road elevation is about 4230 ft (1289 m), for reference. The platform roughly at eye level throughout the marshes is a wave-cut surface left by the regression of the Gilbert lake. It is cut into a ~2-meter-thick deposit of lacustrine sand deposited by the Gilbert lake.

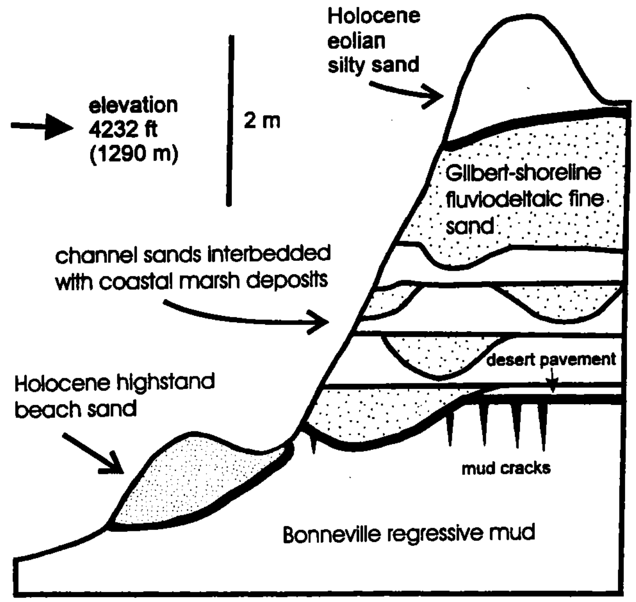

Figure 26. Generalized stratigraphy of road-cut exposures at the Public Shooting Grounds (stop 10). Modified from Currey (1990, fig. 15). Heavy lines represent unconformities. Radiocarbon ages of 10.9, 11.0, 11.6, and 12.0 have been obtained on samples of gastropods and organic-rich sediments from the channel sands and coastal marsh deposits, which were deposited prior to and during the Gilbert transgression (Currey, 1990).

The general stratigraphic sequence in this area (fig. 26) has been described by Currey (1990). Reddish silty sediments at the base of the section are interpreted as late regressive-phase deposits of Lake Bonneville. These are overlain by gray, organic-rich mud and channel sands containing abundant molluscs, which have been dated at 11.9–10.9 ka (Miller et al., 1980; Currey, 1990). The organic-rich mud was probably deposited in a marsh environment, as suggested by the mollusk and ostracode faunas. Sand, interpreted as having been deposited during the transgression to the Gilbert shoreline (20 ft [6 m] above this site), overlies the marsh mud. The Gilbert shoreline was produced between 10.9 and 10.3 ka (Currey, 1990; Benson et al., 1992). All Holocene highstands of Great Salt Lake were lower than the Gilbert shoreline.

Reset mileage to zero and proceed east on Highway 83.

2.0 The Stansbury, Provo, and Bonneville shorelines are prominently displayed to the northeast on Little Mountain.

3.5 Putrid hot springs are common near the road as we drive along the base of Little Mountain. East of Little Mountain, flats produced during the Gilbert regression merge with a broad, low-relief delta plain of the Bear River. East of the town of Corinne, the road drops to the modern flood plain of the Bear River. Bear River probably delivered the largest water and sediment influx to Lake Bonneville.

13.8 Turn left to enter I-15 southbound. Bonneville and Provo shorelines are visible to the east on the face of the Wellsville Mountains. A Gilbert-type delta graded to the Provo shoreline can be seen at the mouth of Box Elder Creek above Brigham City. Extensive quarries mark the delta.

Mile 358. On the east are good views of fault scarps cutting Holocene alluvial fans at the base of the Wasatch Mountains. This segment of the fault has undergone repeated Holocene rupture, but the youngest identified event is 3600 ± 500 years ago (Machette et al., 1991).

Mile 345. To the south is a view of the massive delta of the Weber River. It is composed mostly of silt and fine sand. The delta surface is about at the Provo shoreline.

Mile 340. Views to the west are of Great Salt Lake, Fremont Island, and Antelope Island. Hill Air Force Base lies on a delta surface to the east.

ACKNOWLEDGMENTS

We thank Peter Oviatt for field assistance, Andrei Sarna-Wojcicki, Bill Nash, and Mike Perkins for tephrochronology, Platt Bradbury for diatom identifications, Rick Forester for many discussions about ostracodes over the years, and Genevieve Atwood, Margie Chan, and Paul Link for helpful reviews of the manuscript.

REFERENCES CITED

Adams, T.C., 1938, Land subsidence north of Great Salt Lake, Utah: Bulletin of the Seismological Society of America, v. 28, p. 65–70.

Arabasz, W.J., Smith, R.B., Pechmann, J.C., and Nava, S.J., 1994, Regional seismic monitoring along the Wasatch front urban corridor and adjacent intermountain seismic belt, *in* Jacobson, M.L., compiler, National earthquake hazards reduction program, summaries of technical reports volume XXXV: U.S. Geological Survey Open-File Report 94-176, p. 3–4.

Arnow, Ted, and Stephens, Doyle, 1990, Hydrologic characteristics of the Great Salt Lake, Utah: 1847–1986: U.S. Geological Survey Water-Supply Paper 2332, 32 p., map scale 1:125,000.

Atwood, G., 1994, Geomorphology applied to flooding problems of closed-basin lakes . . . specifically Great Salt Lake, Utah: Geomorphology, v. 10, p. 197–219.

Bates, R.L., and Jackson, J.A., 1987, Glossary of Geology: Third Edition: American Geological Institute, Alexandria, Virginia, 788 p.

Benson, L.V., Currey, D.R., Lao, Y., and Hostetler, S., 1992, Lake-size variations in the Lahontan and Bonneville basins between 13,000 and 9000 ^{14}C yr B.P.: Palaeogeography, Palaeoclimatology, Palaeoecology, v. 95, p. 19–32.

Bills, B.G., and May, G.M., 1987, Lake Bonneville: Constraints on lithospheric thickness and upper mantle viscosity from isostatic warping of Bonneville, Provo, and Gilbert stage shorelines: Journal of Geophysical Research, v. 92, p. 11,493–11,508.

Bond, G.C., and Lotti, R., 1995, Iceberg discharges into the North Atlantic on millenial time scales during the last glaciation: Science v. 267, p. 1005–1010.

Bucknam, R.C., 1979, Northwestern Utah seismotectonic studies: Summaries of Technical Reports, vol. VIII, U.S. Geological Survey, p. 72–74.

Christenson, G.E., Harty, K.M., and Hecker, Suzanne, 1987, Quaternary faults and seismic hazards, western Utah, *in*, Kopp, R.S., and Cohenour, R.E., eds., Cenozoic geology of western Utah: Utah Geological Association Publication 16, p. 389–400.

Crittenden, M.D., Jr., 1963, New data on the isostatic deformation of Lake Bonneville: U.S. Geological Survey Professional Paper 454-E, 31 p.

Currey, D.R., 1980, Coastal geomorphology of Great Salt Lake and vicinity, *in* Gwynn, J.W., ed., Great Salt Lake: A scientific, historical, and economic overview: Utah Geological and Mineral Survey Bulletin 116, p. 69–82.

Currey, D.R., 1982, Lake Bonneville: Selected features of relevance to neotectonic analysis: U.S. Geological Survey Open-File Report 82-1070, 31 p.

Currey, D.R., 1990, Quaternary palaeolakes in the evolution of semidesert basins, with special emphasis on Lake Bonneville and the Great Basin, U.S.A.: Palaeogeography, Palaeoclimatology, Palaeoecology, v. 76, p. 189–214.

Currey, D.R., and Oviatt, C.G., 1985, Durations, average rates, and probable causes of Lake Bonneville expansions, stillstands, and contractions during the last deep-lake cycle, 32,000 to 10,000 years ago, *in* Kay, P.A., and Diaz, H.F., eds., Problems of and Prospects for Predicting Great Salt Lake Levels: Salt Lake City, University of Utah Center for Public Affairs and Administration, p. 9–24.

Currey, D.R., and Burr, T.N., 1988, Linear model of threshold-controlled shorelines of Lake Bonneville: Utah Geological and Mineral Survey Miscellaneous Publications 88-1, p. 104–110.

Currey, D.R., Oviatt, C.G., and Plyler, G.B., 1983, Lake Bonneville stratigraphy, geomorphology, and isostatic deformation in west-central Utah: Utah Geological and Mineral Survey Special Studies, v. 62, p. 63–82.

Currey, D.R., Atwood, G., and Mabey, D.R., 1984, Major levels of Great Salt Lake and Lake Bonneville: Utah Geological and Mineral Survey Map 73, scale 1:750,000.

Currey, D.R., Berry, M.S., Douglass, G.S., Merola, J.A., Murchison, S.B., Ridd, M.K., Atwood, G., Bills, B.G., and Lambrechts, J.R., 1988, The highest Holocene stage of Great Salt Lake: Geological Society of America Abstracts with Programs, v. 20, p. 411.

Eardley, A.J., 1938, Sediments of Great Salt Lake: American Association of Petroleum Geologists Bulletin, v. 22, p. 1305–1411.

Eardley, A.J., and Gvosdetsky, V., 1960, Analysis of Pleistocene core from Great Salt Lake, Utah: Geological Society of America Bulletin, v. 71, p. 1323–1344.

Eardley, A.J., Shuey, R.T., Gvosdetsky, V., Nash, W.P., Picard, M.D., Grey, D.C, and Kukla, G.J., 1973, Lake cycles in the Bonneville basin, Utah: Geological Society of America Bulletin, v. 84, p. 211–216.

Forester, R.M., 1987, Late Quaternary paleoclimate records from lacustrine ostracodes, *in* Ruddiman, W.F., and Wright, H.E., Jr., eds., North America and adjacent oceans during the last deglaciation: Geological Society of America, Geology of North America K-3, p. 261–276.

Green, S.A., and Currey, D.R., 1988, The Stansbury shoreline and other transgressive deposits of the Bonneville lake cycle: Utah Geological and Mineral Survey Miscellaneous Publication 88-1, p. 55–57.

Gwynn, J.W., ed., 1980, Great Salt Lake: A scientific, historical, and economic overview: Utah Geological and Mineral Survey Bulletin 116, 400 p.

Gwynn, J.W., and Murphy, P.J., 1980, Recent sediments of the Great Salt Lake basin: Utah Geological and Mineral Survey Bulletin 116, p. 83–96.

Gilbert, G.K., 1890, Lake Bonneville: U.S. Geological Survey Monograph 1, 438 p.

Kaufman, D.S., and Manley, W.F., in review, A new procedure for determinng enantiomeric (DL) amino acid ratios in fossils using reverse phase liquid chromatography: Quaternary Science Reviews (Quaternary Geochronology)

Lemons, D.R., Milligan, M.R., and Chan, M.A., 1996, Paleoclimatic implications of late Pleistocene sediment yield rates for the Bonneville basin, northern Utah: Palaeogeography, Palaeoclimatology, Palaeoecology, v. 123, p. 147–159.

Light, Adam, and Kaufman, Darrell, 1996, Refinements to the radiocarbon shoreline chronology of Lake Bonneville, Great Basin, USA: EOS v. 77, No. 46, p. 304.

Mabey, D.R., 1986, Notes on the historic high level of Great Salt Lake: Utah Geological Survey, Survey Notes, summer, 1986, p. 13–15.

Machette, M.N., Personius, S.F., Nelson, A.R., Schwartz, D.P., and Lund, W.R., 1991, The Wasatch fault zone, Utah–segmentation and history of Holocene earthquakes: Journal of Structural Geology, v. 13, p. 137–149.

Machette, M.N., and Scott, W.E., 1988, Field trip introduction: A brief review of research on lake cycles and neotectonics of the eastern Basin and Range Province: Utah Geological and Mineral Survey Miscellaneous Publication 88-1, p. 7–14.

Miller, D.M., 1990, Geologic map of the Lucin 4 SW Quadrangle, Box Elder County, Utah: Utah Geological and Mineral Survey Map 130, 13 p., scale 1:24,000.

Miller, D.M., Nakata, J.K., Sarna-Wojcicki, A., and Meyer, C.E., 1992, Neogene tectonic history of northern Utah revealed by depositional, magmatic, and structural features: Geological Society of America Abstracts with Programs, v. 24, no. 6, p. 53.

Miller, D.M., Nakata, J.K., Oviatt, C.G., Nash, W.P., and Fiesinger, D.W., 1995, Pliocene and Quaternary volcanism in the northern Great Salt Lake area and inferred volcanic hazards, *in* Lund, W.R., ed., Environmental and Engineering geology of the Wasatch Front Region: Utah Geological Association Publication 24, p. 469–482.

Miller, D.M., and Langrock, Holly, 1997a, Geologic map of the Monument Peak NE quadrangle, Box Elder County, Utah: Utah Geological Survey Open-File Map OFR 346.

Miller, D.M., and Langrock, Holly, 1997b, Geologic map of the Monument Peak quadrangle, Box Elder County, Utah: Utah Geological Survey.

Miller, D.M., and Langrock, Holly, 1997c, Geologic map of the Locomotive Springs quadrangle, Box Elder County, Utah: Utah Geological Survey Open-File Map OFR 349.

Miller, D.M., and Langrock, Holly, 1997d, Geologic map of the Monument Point quadrangle, Box Elder County, Utah: Utah Geological Survey Open-File Map OFR 348.

Miller, R.D., Van Horn, R., Scott, W.E., and Forester, R.M., 1980, Radiocarbon date supports concept of continuous low levels of Lake Bonneville since 11,000 yr B.P.: Geological Society of America Abstracts with Programs, v. 12, p. 297–298.

Murchison, S.B., 1989, Fluctuation history of Great Salt Lake, Utah, during the last 13,000 years: Ph.D. thesis, University of Utah, Salt Lake City, 137 p.

Nelson, M.G., and Miller, D.M., 1990, A Tertiary record of the giant marmot *Paenemarmota sawrockensis*, in northern Utah: Contributions to Geology, University of Wyoming, v. 28, p. 31–37.

Oviatt, C.G., 1997, Lake Bonneville fluctuations and global climate change: Geology, v. 25, p. 155–158.

Oviatt, C.G., McCoy, W.D., and Reider, R.G., 1987, Evidence for a shallow early or middle Wisconsin lake in the Bonneville basin, Utah: Quaternary Research, v., 27, p. 248–262.

Oviatt, C.G., and Nash, W.P., 1989, Late Pleistocene basaltic ash and volcanic eruptions in the Bonneville basin, Utah: Geological Society of America Bulletin, v. 101, p. 292–303.

Oviatt, C.G., Currey, D.R., and Miller, D.M., 1990, Age and paleoclimatic significance of the Stansbury shoreline of Lake Bonneville, northeastern Great Basin: Quaternary Research, v. 33, p. 291–305.

Oviatt, C.G., Currey, D.R., and Sack, D., 1992, Radiocarbon chronology of Lake Bonneville, eastern Great Basin, USA. Palaeogeography, Palaeoclimatology, Palaeoecology, v. 99, p. 225–241.

Oviatt, C.G., Habiger, G.D., and Hay, J.E., 1994, Variation in the composition of Lake Bonneville marl: A potential key to lake-level fluctuations and paleoclimate. Journal of Paleolimnology, v. 11, p. 19–30.

Robison, R.M., and McCalpin, J.P., 1987, Surficial geology of Hansel Valley, Box Elder County, Utah, *in* Kopp, R.S., and Cohenour, R.E., eds., Cenozoic geology of western Utah: Utah Geological Association Publication 16, p. 335–349.

Sack, D., 1989, Reconstructing the chronology of Lake Bonneville: An historical overview, *in* Tinkler, K.J, ed., History of geomorphology: Unwin Hyman, London, p. 223–256.

Sack, D., 1995, The shoreline preservation index as a relative-age dating tool for late Pleistocene shorelines. An example from the Bonneville basin, U.S.A.: Earth Surface Processes and Landforms, v. 20, p. 363–377.

Scott, W.E., McCoy, W.D., Shroba, R.R., and Rubin, M., 1983, Reinterpretation of the exposed record of the last two cycles of Lake Bonneville, western United States: Quaternary Research, v. 20, p. 261–285.

Smith, R.B., and Luedke, R.G, 1984, Potentially active volcanic lineaments and loci in western conterminous United States, *in* Explosive volcanism: Inception, evolution, and hazards. Washington, D.C., National Academy Press, p. 47–66.

Spencer, R.J., Baedecker, M.J., Eugster, H.P., Forester, R.M., Goldhaber, M.B., Jones, B.F., Kelts, K., McKenzie, J., Madsen, D.B., Rettig, S.L., Rubin, M., and Bowser, C.J., 1984, Great Salt Lake and precursors, Utah: The last 30,000 years. Contributions to Mineralogy and Petrology, v., 86, p. 321–334.

Thompson, R.S., Toolin, L.J., Forester, R.M., and Spencer, R.J., 1990, Accelerator-mass spectrometer (AMS) radiocarbon dating of Pleistocene lake sediments in the Great Basin: Palaeogeography, Palaeoclimatology, Palaeoecology, v. 78, p. 301–313.

U.S. Geological Survey, 1987, Great Salt Lake and Newfoundland evaporation basin. Experimental edition 1:250,000-scale satellite image map: U.S. Geological Survey, Denver, CO.

Williams, S.K., 1994, Late Cenozoic tephrochronology of deep sediment cores from the Bonneville basin, northwest Utah: Geological Society of America Bulletin, v. 105, p. 1517–1530.